HELSINGIN YLIOPISTO
HELSINGFORS UNIVERSITET
UNIVERSITY OF HELSINKI

Hydrological changes in subarctic Russian peatlands during the last millennia due to climate change

University of Helsinki
Faculty of Biological and Environmental Sciences
Environmental Change and Global Sustainability Master's Programme

Master's Thesis

Agneta Boxström

May 2021

Faculty: Biological and Environmental Sciences

Degree programme: Master's Programme in Environmental Change and Global Sustainability

Study track: Environmental Change

Author: Agneta Boxström

Title: Hydrological changes in subarctic Russian peatlands during the last millennia due to climate change

Level: Master's thesis

Month and year: 05/2021

Number of pages: 54

Keywords: Peatlands, climate change, testate amoeba, proxy, carbon dynamics

Supervisors: Minna Väliranta & Matthew Amesbury

Where deposited: Helsinki University Library, Viikki

Additional information:

Abstract: Northern boreal peatlands form one of the biggest carbon pools in the biosphere, thus having great potential to cause major changes to the global carbon cycle. The ongoing recent warming may affect the carbon dynamics though factors, such as, vegetation, hydrology and permafrost balance. As the future is still uncertain there are no definitive answers on how the peatlands will react in the future. Fortunately, moisture sensitive organisms such as, bryophytes and testate amoeba is preserved in the peat and can therefore be used to reconstruct past climatic shifts.

In this thesis I studied palaeohydrology and peat accumulation over the last two millennia, from three peat cores originating in a permafrost peatland in Rogovaya, Russia. I used testate amoeba as a proxy of past moisture conditions and plotted the taxa composition of each core against ^{14}C and ^{210}Pb dated samples, to reconstruct past moisture shifts. The results were also supplemented by plant macrofossil and carbon accumulation data for more robust results.

Of the three cores, Rog11 provided the oldest testate amoeba dataset by reaching the Dark Ages Cold Period. During this period there were indications of dry moisture conditions followed by a wet Medieval Warm Period. The Little Ice Age gave indications of a drying trend, while toward the end of the LIA Rog8 indicated opposite moisture conditions. From the end of the LIA onwards a general trend of drying and increased carbon accumulated is noted. Yet, during the last decade the trend has turned. The wet shift might indicate that the threshold for the peatland has been reached and the amount of melting permafrost has exceeded the evapotranspiration rate.

As a conclusion my result indicates that the dynamics of both hydrology and carbon are complicated processes affected by both autogenic and allogenic factors, therefore causing large variability even on a local scale. The absence of widely spread observations of the most recent wet shift also indicates that the response of the peatland to the recent warming might be unequal. To rectify this situation, continued research is crucial, so that we can increase our understanding of climate-peatland interactions.

Fakultet: Bio- och miljövetenskapliga fakulteten

Utbildningsprogram: Magisterprogrammet i miljöförändring och global hållbarhet

Studieinriktning: Miljöförändring

Författare: Agneta Boxström

Arbetets titel: Hydrologiska förändringar i en subarktisk rysk torvmark under de senaste två millennierna på grund av klimatförändring

Arbetets art: Magisteravhandling

Månad och år: 05/2021

Sidantal: 54

Nyckelord: Torvmarker, klimatförändring, testate amoeba, proxy, koldynamik

Handledare: Minna Väliranta & Matthew Amesbury

Förvaringsställe: Helsingfors Universitetsbibliotek i Vik

Övriga uppgifter:

Sammandrag: De boreala och arktiska torvmarkerna utgör tillsammans en av de största kolreservoarerna i biosfären, vilket leder till att deras potentiella inverkan på det globala kolkretsloppet är stort. Den antropogena klimatförändringen kan påverka kolets kretslopp genom olika faktorer, såsom vegetation, hydrologi och permafrostdynamik. Den oförutsägbara framtiden orsakar bristfällig kunskap om hur torvmarkerna kommer att utvecklas i framtiden. Fuktkänsliga organismer såsom mossor och testate amoebae lagras i torven, och genom att studera dem kan man rekonstruera forna klimatförändringar, vilket bidrar till ökad kunskap om pågående klimatförändringen.

I den här avhandlingen har jag studerat förändringar i de paleohydrologiska förhållandena och ansamlingstaken av kol för de senaste två millennierna i en torvmark i Rogovaya, Ryssland. Jag använde testate amoeba som en indikatorart för fuktighetsförhållandena och kombinerade dessa resultat med daterade torvsampel (^{14}C och ^{210}Pb), för att rekonstruera de forna variationerna i klimatet. Växt makrofossil och kolansamlingsdata inkluderades för att få mer omfattande resultat.

Av de tre insamlade torvpelarna, som studerades i denna avhandling, bidrog Rog11 med data som daterades till tidig medeltid, därmed det äldsta samplet. Under den här tidsperioden antyder resultaten att förhållandena varit relativt torra med påföljande våta förhållanden under den medeltida värmeperioden. Under den lilla istiden börjar det torka upp igen men mot slutet kan man se motsatta antydningar i data för de andra samplen. Efter den lilla istiden inleds en period som markeras av en klar trend av upptorkning och en ökad ansamlingstakt av kol. Denna trend har dock svängt under det senaste årtiondet. Förändringen i trenden från torrt till våt kan antyda att torvmarkens tröskelvärde har nåtts och att smälttaketen för permafrosten har blivit snabbare än evapotranspirationen.

Mina resultat antyder att dynamiken för både hydrologin och kolbalansen är komplexa processer och de påverkas av både inre och yttre faktorer, vilket även orsakar variationer på en lokalnivå. Bristen på geografiskt välutbredda observationer av den senaste trenden mot fuktigare förhållanden antyder att torvmarkens respons till den senaste klimatförändringen inte är likadan överallt. Fortsatt forskning är viktig för att förbättra vår kunskap om interaktioner mellan klimatet och torvmarkerna.

1. Introduction

The Northern boreal peatlands are estimated to cover an area of 4.0 million km^2 and they form one of the biggest carbon pools in the biosphere, as approximately 50 % of the peat dry weigh is carbon (McGuire et al. 2009; Loisel et al. 2014; Treat et al. 2016). The carbon stored in the peat, represents about 1/3 – 1/2 of the global soil carbon pool and therefore it has great potential to cause major changes to the global carbon cycle, if the stored carbon is being released. As elevated CO_2 levels in the atmosphere is one of the main drivers of the modern global climate change (IPCC, 2014) is it crucial to know how the carbon pool in peatlands have reacted to climate change in the past (Charman et al. 2013). Peatlands can be used as an archive to study carbon accumulation patterns and their link to climate. One of the driving factors in carbon accumulation is moisture, and this can be studied by modelling the estimated water table depth (WTD) changes with the help of indicator species or proxies, such as, testate amoeba or plant macrofossils.

1.1 Peatlands

Peatlands can be defined in various ways and in Finland the most common method is a classification based on vegetation (Cajanderian tradition). Peatlands can also be defined according to their function for geological, agricultural or forestry purposes. Ecologically peatlands are ecosystems sustained by a humid climate and a high water-table, where partially decomposed organic material is accumulated as peat (Laine & Vasander, 1996). In geology, at least 40 cm of peat defines a peatland (Charman, 2002). Peatlands can be divided into two groups depending on their water source, and thus nutrient source. Ombrotrophic peatlands (bogs) are nutrient poor, due to their convex shape. As a result, they have lost a connection to the groundwater and therefore get all their water and nutrients from the atmosphere. Minerotrophic peatlands (fens and swamps), on the other hand, are nutrient rich because the water running through them have been enriched by mineral soils, as the water has flown through the upper parts of the catchment or is coming from ground water (Laine & Vasander, 1996).

Apart from the water and nutrient availability there are other factors that separate the ombrotrophic peatlands from minerotrophic. In ombrotrophic peatlands the pH is usually very low (<4) and therefore ombrotrophic peatlands are regarded as extreme habitats, with a combination of nutrient availability and pH. As the pH variability in minerotrophic peatlands is rather large, they have been

divided into subcategories according to their pH level: oligotrophic (4.5), mesotrophic (5.5) and eutrophic (5.5 – 7.5) (Laine & Vasander, 1996).

One of the most important factors that separates ombrotrophic peatlands from other ecosystems is the massive occurrence of *Sphagnum*-mosses. The dominance of *Sphagnum*-mosses can be explained by several reasons 1) they are able to manipulate their surrounding by producing organic acids and 2) they are not consumed by any animal. (Laine & Vasander, 1996).

Peat formation includes phases where the vegetation on the top goes through a decomposition process both in aerobic and anaerobic conditions. During these phases the plant material loses its physical structure, some of its organic material and there is a change in the chemical state. The decomposition of the organic material is fastest in the acrotelm, which is a layer of peat at the surface, where aerobic decomposition is possible. In the acrotelm about 80 – 95 % of the plant biomass is decomposed and the rate of decay is affected by factors, such as, the chemical composition of the vegetation, pH and the availability of oxygen and nutrients. In the acrotelm the most important decomposers are oxic bacteria and they produce carbon dioxide (CO_2). In the catotelm, which is an anaerobic environment underlying the acrotelm, the bacteria mainly produce carbon dioxide and methane (CH_4). In this layer of the peat column, the effectivity of the bacteria is affected by factors, such as, temperature, moisture and vegetation composition (Laine & Vasander, 1996).

1.1.1. Carbon accumulation and storage in peatlands

Peatlands can act both as a sink or a source of carbon and it has been estimated that high latitude peatlands have accumulated about 500 GtC during the Holocene, with an average speed of 20 – 30 g of C/m^2/yr (Yu et al. 2011; Loisel et al. 2014; Mathijssen et al. 2016). Studies have shown that the tundra region, in the Arctic, functions as a C source during dry and mesic conditions and as a C sink during wet conditions (McGuire et al. 2009). Fens also generally emits more CH_4 than bogs (Alm et al. 1999; Heiskanen et al. 2021). Peatlands in the Northern Hemisphere are still considered as sinks even though they, due to their dualistic function, apart from CO_2 also emits between 15 – 50 Tg of CH_4 annually to the atmosphere (McGuire et al. 2009; Mathijssen et al. 2016). This balance may, however, shift in the future due to climate change (McGuire et al. 2009; Charman et al. 2013; Gallego-Sala et al. 2018). It has, however, been estimated that if the climate conditions stay the same, then high-latitude peatlands could potentially store up to 875 ± 125 PgC (Alexandrov et al. 2020).

There are large variations in, both short- and long-term, annual C budgets, and the most important limiting factor for C sequestration is sunlight, due to photosynthesis (Gallego-Sala et al. 2018). The sum of the photosynthetically active radiation over the growing period (PAR0) have been shown to statistically best explain C accumulation in the north (Charman et al. 2013; Gallego-Sala et al. 2018). Some carbon is also lost from peatlands, by either surface runoff (dissolved organic carbon, DOC), fires or erosion (Laine & Vasander, 1996; Mäkilä & Saarnisto, 2008; Sillasoo et al. 2011).

In Finland, where about 30 % of the total land area is classified as peatlands, the estimated value for the carbon being stored in year 2000 was ~5304 Tg, with an annual sink of 2.9 – 3.6 TgC (Turunen, 2008).

1.2. Peatlands in the Arctic region

In the subarctic region, where the annual mean temperature in below 0 ºC and the permafrost is widely spread, so called palsa mires are common (Brown et al. 1998; Treat et al. 2016). Palsa mires are a combination of minerotrophic aapa mires and ombrotrophic bogs. The palsa hummocks themselves are classified as bogs and the wet surface between the mounds as aapa mires. Because water is needed for palsas to form is it also common for small creeks to cross the palsa mire. However, too much water is fatal for the palsas and therefore can the ice core in the palsa thaw if the mire is flooded for an extended period of time (Seppälä, 2011). Palsa mires can be found in the zone of discontinuous permafrost in the circumpolar region of the Northern Hemisphere (Seppälä, 2011). Of the two palsa types, single palsa mounds generally grows higher (up to 12 m), while the much larger palsas, called plateaus, can be found in the northern parts of this region (Lagarec, 1982; Charman, 2002; Seppälä, 2011). Palsa establishment is in the south limited by the natural limit for permafrost formation, but other factors, such as, vegetation, soil composition, precipitation and wind conditions are also important. According to Seppälä (1986) low air temperatures combined with low precipitation and a thin snow cover are the most important limiting factors for palsa establishment. While, a spatial analysis of palsa mires in the northern Fennoscandia concluded that a low annual precipitation (<450 mm) and a mean annual air temperature between -3 °C and -5 °C, are optimal conditions for palsa establishment (Luoto et al. 2004).

Palsas and permafrost aggradation have a great impact on peatlands, because they can alter the hydrology, thus affecting the composition, productivity and decomposition of the vegetation and therefor the C accumulation rates (Treat et al. 2016). Another factor that also changes due to

permafrost aggradation is topography. When palsa rises above the surface of the peatland, a dry area is formed. This area has its own vegetation, is more prone to wildfires and have an increased decomposition rate, which lowers the overall C accumulation rates of the peatland compared to unfrozen peatlands (Camill et al. 2009; Treat et al. 2016).

Palsas are formed due to permafrost movements and it is thought that they have a circular life span (Seppälä, 1986). According to Seppälä (1986) there are six stages in a palsas life-cycle: 1) A locally thin snow cover facilitates cold penetration that goes deep enough that summer temperatures are not able to melt the frozen ground, a small hump is formed. 2) During following winters, the frost penetrates deeper and the small hump grows in size. As the hump grows larger the effect of the wind, in keeping the top snow-free, grows. 3) When the frozen core of the palsa reaches the till or silt layers at the bottom of the peatland, the mature life stages of the palsa begins. 4) After this, the degradation of the palsa starts. This happens either slowly from the bottom, by melting, or much faster from above by erosion. 5) Dead palsas are unfrozen remains of the collapsed much larger dome that usually forms a low ridge, round pools and pool groups or open peat surfaces with no vegetation. 6) A new palsa can be established from such a place after a renewed phase of peat formation (Seppälä, 1986).

1.3. Climate change

During the last 2 millennia there have been four major climatic periods in addition to the post-industrial warming (PIW) that we are experiencing now. The Roman Warm Period (RWP) and Medieval Climate Anomaly (MCA) are considered to be periods with temperatures above average, while the Dark Age Cold Period (DACP) and Little Ice Age (LIA) are considered to be periods with temperatures below average. Of these periods, MCA and LIA are the most resent and therefore also the most intensively studied. However, scientists have noticed that the exact peak of each warm and cold period varies geographically and therefore, it is challenging to establish exactly defined climatic periods that are valid for the whole world (Mann, 2002; PAGES 2k Consortium, 2013). One suggestion for a potential division based on data from the extra-tropical Northern Hemisphere is: RWP (anno domini (AD) 1 – 300), DACP (AD 300 – 800), MCA (AD 800 – 1300), LIA (AD 1300 – 1900) and PIW (AD 1900 onwards) (Ljungqvist, 2010). The exact reasons behind these climate anomalies are to some extent still unresolved, but the assumption is, that they are driven by a combination of factors, whose mechanisms can be connected to the solar activity or volcanic eruptions (Mann, 2002; PAGES 2k Consortium, 2013).

The recent on-going warming is mostly caused by anthropogenic greenhouse gas (GHG) emissions caused by factors, such as, population size, economic activity, lifestyle, energy use, land-use patterns, technology and climate policy, which consequently increases CO_2 levels in the atmosphere (IPCC, 2014). An area-weighted average estimated that 1971 – 2000 has been the warmest 30-year period in nearly 1400 years (PAGES 2k Consortium, 2013). And that the global mean temperature for the decade 2006 – 2015 was 0.87 °C warmer than the average for 1850 – 1900. It has also been estimated that the anthropogenic global warming is currently increasing at a speed of 0.2 °C per decade. However, in areas, such as, the Arctic region the experienced warming is two or three times greater than the global average (IPCC, 2018). To predict the future, IPCC have made up four possible scenarios for the 21st century called Representative Concentration Pathways (RCP). They take into account GHS emissions and atmospheric concentrations, air pollutant emissions and land-use. Of the two extremes RCP8.5 represents the business-as-usual scenario, which will lead to an estimated increase of 7.5 °C to the global mean surface temperatures if procedures do not change. The RCP2.6 scenario, on the other hand, strives to keep the global warming below 2°C above pre-industrial temperatures (IPCC, 2014). However, during the 21st conference of the parties of the UNFCCC (United Nations Framework Convention on Climate Change) in Paris did the representatives of 196 parties negotiated the so-called Paris agreement. The goal for this agreement is to make an effort to restrict the temperature increase to 1.5 °C above pre-industrial temperatures (UNFCCC, 2020).

1.3.1. Peatlands and climate change

Because peatlands can be found all over the Northern Hemisphere is it challenging to predict any uniform consequences of the climate change on peatlands. However, two competing scenarios for the future have recently been proposed for peatlands in the Northern Hemisphere: 1) A warmer climate will lead to dryness where decomposition will exceed the productivity (Swindles et al. 2019). 2) A warmer climate with enough moisture will lead to increased productivity, but only for the following 100 years (Gallego-Sala et al. 2018) after which processes in the tropical peatlands will mitigate accelerated C uptake of the high-latitudes.

The difference between these two scenarios is water availability, supporting Charman, (2002) conclusion where he stated: “Hydrological change is probably the most important and universal response of peatlands to climate change”. According to him, peatlands can be affected by climate change in four different ways. 1) Location: the centre of a palsa mire area is less sensitive to changes

than the margin (Zhang et al. 2018c). 2) Seasonal variation: Some areas are more sensitive to changes during a particular season than others. 3) Type of peatland: Minerotrophic peatlands are less sensitive than bogs to changes in precipitation conditions, while they are more sensitive to a drop in the WTD (Kokkonen et al. 2019). 4) The strength and impact of autogenic (internal) and other allogenic (external) factors: climate change usually only accelerates or retard the effect of other factors on peatlands e.g., peatland fires (Charman, 2002). Because these factors, combined with carbon accumulation, hydrology and vegetation form a complex feedback network (Swindles et al. 2015b) can either of the two scenarios mentioned above come true.

Interlinked changes to temperature and moisture conditions will cause changes to the vegetation, which instead will lead to significant changes to the C accumulation rates (Charman et al. 2013; Treat et al. 2016; Gallego-Sala et al. 2018; Zhang et al. 2018b). It has, for example, been estimated that the net primary production (NPP) will increase in high-latitude ecosystems due to a warmer and longer growing-period, which will result in higher C accumulation rates in these areas (Charman et al. 2013; Gallego-Sala et al. 2018). This change will be most prominent in areas with bryophyte vegetation because they start to photosynthesize when the temperature rises above 0°C. However, higher temperatures also increase microbial activity, which leads to a higher decomposition rate for the peat (Charman et al. 2013). The change in vegetation cover can also be noticed in the thickness of the active layer of the permafrost. Higher shrubs generally indicate, a thinner active layer, while the active layer usually is thicker under bare peat (Seppälä, 2011).

It has been noticed that areas of permafrost have retarded toward the poles, leaving degradation features, such as, thaw lakes, increased active layer thickness and permafrost free zones in its wake (Turetsky et al. 2019; Sim et al. 2021). The future of permafrost is still uncertain, but many believes that it will slowly continue to degrade during the next century. One factor that for example, drastically can affect the rate of permafrost degradation are wildfires. They not only locally melt the surface permafrost and releases huge amount of CO_2 to the atmosphere, but they also destroy the protective layer of organic matter on top of the deeper layers of permafrost (McGuire et al. 2009). Another factor that can be more important in the future, especially for palsas, is a higher amount of precipitation in the summer. A higher precipitation leads to wetter peatlands which more easily thaws the ice core, opposite to a layer of dry insulative peat (Seppälä, 2011).

When considering the carbon balance of peatlands, permafrost thaw can increase decomposition of previously frozen organic soil and therefore release greenhouse gases to the atmosphere. Permafrost

thaw is also associated with an increase in the productivity, higher methane emissions and higher rates of C accumulation (Treat et al. 2016; Zhang et al. 2018b). Another factor that is affected by permafrost thaw is the surface hydrology or WTD of the peatland. It has been estimated that the WTD will fall in areas with hummocks, lawn, swamps and pools. While the WTD might rise on plateau palsas due to permafrost thaw (Willis et al. 2015). Depending on, if the peatland is drying or getting wetter the carbon balance pathways appear opposite. A drying peatland can promote decomposition and decrease carbon accumulation, whereas a higher water table can prevent the overall decomposition and increase the amount of CH_4 being released (McGuire et al. 2009; Willis et al. 2015; Zhang et al. 2018b).

Because the permafrost is degrading, also the palsa mires are degrading. Therefore, different models on how degrading permafrost peatlands will respond to increasing temperatures have been proposed. 1) Intact: Pristine permafrost peatlands are sinks of CO_2. 2) Desiccation: The surface of the palsa starts to dry due to higher temperatures, leading to greater evapotranspiration, desiccation of the peat surface, a slow lingering of the WTD and a high level of decomposition. 3) The threshold: Continued drying leads to peat shrinkage and the peat surface begins to crack. During phases 2 and 3 both CO_2 and N_2O will be released from the active layer and the newly thawed peat, while CH_4 remains neutral. 4) The collapse: Fast degradation of permafrost causes palsas to collapse rapidly and the meltwater saturates the surrounding peatland. After the collapse fens and bogs are CO_2 sinks and CH_4 sources while thermokarst lakes are sources of both CO_2 and CH_4 5) Stabilization of postthaw peatlands: Over time the CH_4 source grows weaker and lakes that were CO_2 sources turn to sinks (Swindles et al. 2015b; Hugelius et al. 2020)

Arctic fen: All the permafrost has melted, and the peatland is now influenced by surface and groundwater inflow from surrounding peatlands. The last stage has the potential for large carbon sequestration due to high productivity and rapid peat accumulation, however, elevated methane emissions are also likely (Swindles et al. 2015b)

1.4. Testate amoeba (TA)

Testate amoeba (TA) are microscopic 5 – 250 μm (Warner, 1988) unicellular organisms (protozoa) that form a shell or test. They are considered as largely cosmopolitan organisms (Charman et al. 2000) and they can be found in different kinds of wetlands, including peatlands (Amesbury et al. 2016). In peatlands TA live in the water film on the surface of the host substrate and after their death, the tests

are preserved in peat (Turner et al. 2013). The tests of TA are taxonomically distinctive (Tolonen et al. 1992). They are either formed of secreted material, smooth or plated (idiosomic) or of particles, which they gather from the environment and then glue together with secretion (xenosomic). Other characteristics for taxon recognition are the morphology, composition and size of the test. In living TA, the pseudopodia, which they use for feeding, movement and attachment, and some nuclei structures are the main parts that differ them from other groups in their class. These features are however unavailable for fossilized samples due to degradation (Charman et al. 2000).

TA have an important role in the microbial ecosystem because they enhance the nutrient recycling in the peat by consuming bacteria, protozoa, micro-algae, fungi and micrometazoa. The community composition of TA is affected by both biotic and abiotic factors such as moisture, pH and nutrient availability (Turner et al. 2013) and therefore they react rapidly to climate change. The strength of each factor varies, depending on whether the peatland is ombrotrophic or minerotrophic (Zhang et al. 2018a). According to Zhang et al. (2018) the impact of non-hydrological factors, such as pH, increase when the nutrient availability grows.

The ecological coupling between moisture and taxonomic composition has been known for long (Tolonen, 1966; Tolonen et al. 1992) and later confirmed (Charman et al. 2007; Amesbury et al. 2016). Therefore, both qualitative and quantitative methods have been developed to interpret and model this connection (Charman et al. 2000). According to Charman et al. (2000) there are four major ways to interpret the results qualitatively. You can either do a general subjective interpretation based on existing knowledge (Tolonen, 1966), use indicator taxa (Aaby, 1976), divide the TA diagram into wetness zones (Warner, 1988) or produce a semi-quantitative illustrations of wetness changes (Beyens, 1985). Of these, the first method is the simplest, while the last one combines qualitative information on hydrological preferences with quantitative percentage data for each taxon. This makes the last approach an intermediate way between the qualitative and quantitative methods (Charman et al. 2000). A procedure for quantitative reconstruction of past environmental variables based on fossil assemblages, was presented for the first time in 1971 (Birks, 1995). Since then, the so-called transfer or calibrated functions have evolved as computer programs have become more sophisticated. The modern models strive to reconstruct past shifts in hydrology based on fossil data (Swindles et al. 2015a; Amesbury et al. 2016) by using a modern training set that is assumed as representative for past communities prevailed throughout time. Yet, studies that compare other proxies such as pollen, tree rings, plant macrofossils or stable isotopes to the TA data are usually recommended (Lamentowicz et al. 2008).

1.4.1. Testate amoeba as hydrological proxy group

Most TA taxa have a water table depth (WTD) optimum, around which they are distributed (Tolonen et al. 1992), however, this preference may vary if the amount of nutrients in the peatland rises (Zhang et al.2018). The most useful taxa that occupy a narrow niche along the hydrological gradient are *Amphitrema wirghtianum, Archerella flavum, Archella discoides* type, *Hyalophenia subflava, Trigonopyxis arcula* type and *Assulina muscorum* (Turner et al. 2013). And this confirms the idea of Tolonen et al. (1992) that if we can define the ecological tolerance range of some TA taxon, then they can provide valuable palaeoenvironmental information.

When looking at the taxonomic composition according to their preference of WTD, then *H. subflava* is considered a taxon that prefers the driest places. Other taxa that also can be included in the dry category are *T. arcula* type, *Trinema-Corythion* type, *Alabasta militaris, Phryganella acropodia* type, *Nebela tincta* and *Bullinaria indica* (Charman et al. 2000). Later research also includes *Euglypha strigosa* type, *Assulina muscorum* and *Nebela flabellum* in this category (Swindles et al. 2015a).

On the wet end of the WTD gradient, taxa from the genus *Arcella* are common, with example taxa, such as *A. catinus* type, *A. artocrea, A. flavum* and *Amphitrema wrightianum.* Other taxa that also occur at moister locations are taxa from the *Difflugia* genus, *Hyalophenia elegans, Hyalosphenia papilo* and *Placocista spinosa* type (Charman et al. 2000). The taxa *Difflugia pristis* type, *Pseudodifflugia fulva* type and *Centropyxis aculeata* type have also been added to this category (Swindles et al. 2015a).

Intermediate taxa that have a moisture preference from either intermedium to dry or intermedium to wet are difficult to categorize. Because depending on the author and when the study is published the line between the dry/wet category and the intermediate category varies. For example, taxa from the *Assulina* and *Euglypha* genus have been included in the intermediated category by one study (Charman et al. 2000). While another has moved *A. muscorum* to the dry category because it preferers dryer habitats compared to *A. seminulum* (Swindles et al. 2015a). This kind of change has also happened to other taxa, such as, *E. strigosa* type, *A. militaris* and *Nebela tincta.* But, for *E. rotundata* type and *E. tuberculata* type there has been no change of category between these two publications

(Charman et al. 2000; Swindles et al. 2015a). Taxonomic re-arrangements keep exciting exist because, to date, ecology of many taxa is still unresolved. This is reflected as a constant reorganization of the taxonomy when new information arises. Because the taxonomy is constantly changing is this a factor that must be considered when looking at older studies.

1.5. Study background and research hypotheses

This thesis is part of a larger research project funded by the Academy of Finland, coordinated by docent M. Väliranta and carried out at the Environmental Change Research Unit (ECRU). The aim of the project is to expand our knowledge of how northern permafrost peatlands are reacting to the on-going climate change, by using a multiproxy approach. The study is motivated by the pressure of future climate change to high-latitude peatlands in general. At the moment there are two main scenarios for the future of peatland due to climate change (Gallego-Sala et al. 2018; Swindles et al. 2019). While the former predicts increases in C uptake due to warming, the latter is reporting of extensive drying of peatlands. This could lead to C release to the atmosphere. In these, the crucial factor is the amount of moisture in the peatland ecosystem. Therefore, one of the larger sub-projects aims to study past and present moisture component with the help of TA. These analyses are supplemented by plant macrofossil data, and the associated carbon dynamics data from each peatland analysed by other team members, and these are outside of my thesis scope.

My thesis is based on TA analyses of three peat sections from Rogovaya, Nenets Autonomous District in Russia. I am using TA to reconstruct the past WTD changes which have occurred in this plateau permafrost peatland. The location of the study site was chosen because palaeoecological studies made in this area are scarce, therefore this data can enlarge our understanding of how the peatlands are and have been reacting to climate change in European side of northern Russia (Oksanen et al. 2001; Zhang et al. 2017), especially over the last millennia. I have also plant macrofossil and carbon data at my disposal for comparison, provided by other team members partaking in the same project.

My hypotheses for the study are the following:

1) Past climate phases are recorded in the peat as changes in the moisture conditions
2) Past changes in moisture conditions are reflected in testate amoeba community shifts

3) Fossil testate amoeba assemblage can provide quantitative estimates of past peatlands water table changes

2. Material and methods

My thesis is based on three peat cores (Rog2, Rog8 and Rog11), collected from a permafrost peatland in Rogovaya, Nenets Autonomous District, Russia (10 – 11.8.2018). A total of 16 cores from three different transects were cored. Transect one consist of samples Rog1 – Rog6, the second transect of the samples Rog7 – Rog10 and the third transect of the samples Rog11 – Rog16, which means that my samples are from different transects. The samples were taken with a box-corer that takes surface samples of a maximum depth of 60 cm.

2.1. Study site

Figure 1. Exemplary view over the study area in Rogovaya, Russia. Photo © Tarmo Virtanen.

The study site is located in Rogovaya, Nenets Autonomous District, a few kilometres northwest of the border of the Komi Republic, Russia (Figure 2). In general, the current mean temperature in the region in the NE Russia is still below 0°C, but more and more often individual years approach 0°C (Naryan-Mar meteorological station covering the period: 1961 – 1990, Vorkuta meteorological stations covering the period 1977 – 2006; Zhang et al. 2018c). The mean temperature of the warmest month, July is about 13.0°C and the lowest temperature for each month is below zero, except for some years in July and August. Annually, the mean precipitation is about 500 mm, of which about 250 mm falls as snow. The average snow depth in April is about 0.65 m and the average snow cover lasts for about 230 days (Petrun and Vokuta meteorological stations; Oksanen et al. 2001).

The study site is located in the forest tundra ecotone and therefore covered by typical geological formations found on the tundra, such as, permafrost plateaus and palsas (Figure 1). The vegetation on the plateaus consists mainly of lichen, mosses and shrubs. Between the plateaus and along the rivers, small patches of forest with spruce (*Picea abies*) and some mountain birch (*Betula pubescens* subsp. *czerepanovii*) grow on sandy grounds. Tall willow shrubs can also be found in the riversides, while higher vegetation, such as, trees and taller shrubs are almost non-existent on the peat plateaus. The peatland itself is a very typical example of the area with a large uplifted peat plateau covered by smaller wet depression and shallow wet cracks. The different peat plateaus are about 1.5 – 2 m high and up to 100 m long. The plateaus are separated from each other by small fens or water canals. There are many thermokarst formations in the area and collapse features are common around the ponds. (Oksanen et al. 2001)

2.2. Samples

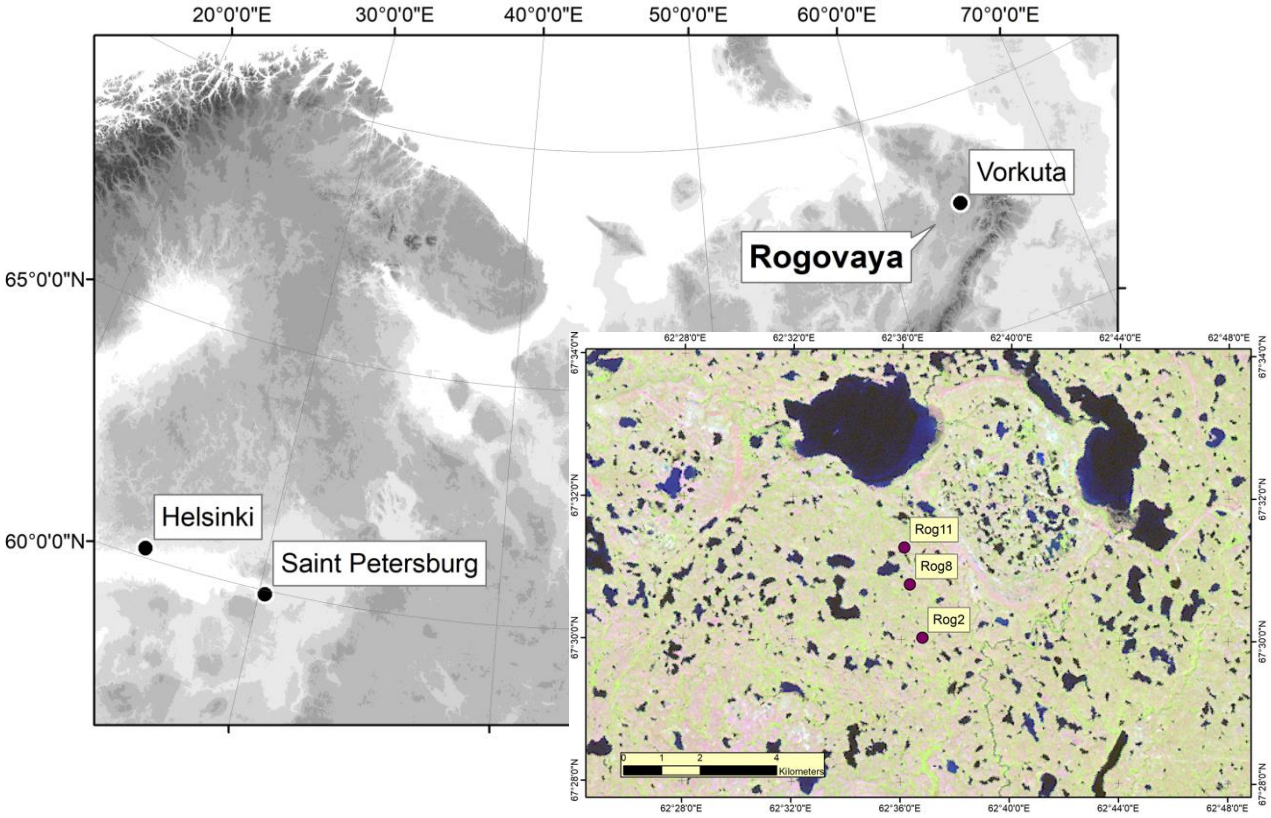

Figure 2. Map over the study site and coring locations.

Table 1. Information of the study site and habitat conditions.

	Rog2	Rog8	Rog11
N	67°19.662`	67°19.707`	67°19.738`
E	062°36.471`	062°36.019`	062°36.640`
Water table depth (cm)	17	12	20
Permafrost depth (cm)	47	35	50
Collected core depth (cm)	40	35	49

2.2.1. Rog2

The coordinates for Rog2 is N 67°19.662`, E 062°36.471` (Figure 2). The length of the collected sample was 40 cm with and estimated active layer thickness of 47 cm and a WTD of 17 cm (Table 1). At the coring site the vegetation consisted mainly of different *Sphagnum* species such as *S. fuscum* and *S. rubellum/S. capillifolium* but also lichen from the *Cetraria* spp., *Rubus chamaemorus* and *Rhododenron tomentosum* (Figure 3).

Figure 3. Newly cored Rog2 on site. Photo © Sanna Piilo.

The topmost 3 cm of the peat core consisted of living *Sphagnum* sp. From 3 to 10 cm the *Sphagnum* sp. was more decomposed, and some roots were also present. Between 10 to 25 cm the *Sphagnum* sp. was brown and decayed. 25 – 35 cm there was only a dark strip and the rest of the core downwards was highly humified with brown peat.

2.2.2. Rog8

The coordinates for Rog8 is N 67°19.707`, E 062°36.019` (Figure 2). The length of the collected sample was 35 cm with and estimated active layer thickness of 35 cm and a WTD of 12 cm, which makes it both the most shallow and wettest of the cores included in my thesis (Table 1). According

to the fieldnotes Rog8 had also one of the thinnest active layers among all cores taken, measuring only 3 cm thicker than the most swallow core. Around the coring place the vegetation consisted of the mosses *S. fuscum* and *Polytrichum* sp. and the lichens *Cladonia* ssp. and *Cetraria* sp. Among the vascular plants *R. chamaemorus, Vaccinium uliginosum, R. tomentosum* and *Betula nana* could be found at the site (Figure 4).

Figure 4. Newly cored Rog8 on site. Photo © Sanna Piilo.

Of the cores' total length only the topmost 2 cm consisted of living *Sphagnum* while the rest of the core consisted of varying degree of degraded *Sphagnum* or peat. Centimetres 2 – 7 consisted of dead *Sphagnum* remains and 7 to 12 of darker peat with some roots. Between 12 to 21 cm the peat consisted of a lighter *Sphagnum* species and the rest of the core of dark brown fen peat.

2.2.3. Rog11

The coordinates for Rog11 is N 67°19.738`, E 062°36.640` (Figure 2). The length of the collected sample was 49 cm with and estimated active layer thickness of 50 cm and a WTD of 20 cm, which makes it the driest core and the one with the thickest active layer chosen for my thesis (Table 1). According to the fieldnotes the maximum active layer could, however, not be established but they expect it to be over 60 cm. The vegetation at the coring site consisted mainly of *Sphagnum fuscum*

and *S. rubellum*/*S. capillifolium*, but also lichen from the *Cladonia* genus and vascular plants, such as, *R. chamaemorus*, *Andromeda polifolia* and *Vaccinium oxycoccos* (Figure 5).

Figure 5. Newly cored Rog11. Photo © Sanna Piilo.

The maximum depth of the living *Sphagnum* was at this site 2.5 cm. From 2.5 to 8 cm there were dead *Sphagnum* remains, while the peat between 8 to 13 cm consists of a darker *Sphagnum* with roots. At approximately the same depth as in Rog8 (12 – 21 cm) the peat in Rog11 also consisted of a lighter *Sphagnum* between 13 – 23 cm. At the bottom of the core the peat becomes more decomposed with chocolate brown peat from 23 – 40 cm and dark almost black peat with *Menyanthes* sp. seeds from 40 – 49 cm.

2.3. Sample analyses

2.3.1. Testate amoeba (TA)

The analysing process started by diving the peat cores into smaller subsamples. The slices were 1 cm thick, which gave us the samples Rog2 1 – 40, Rog8 1 – 35 and Rog11 1 – 48. For the TA analysing we further prepared 20 samples from each core of every second cm starting with 1 cm = 0 – 1 cm, according to a modified version of Booth et al (2010) standardized method. For each subsample we

used 2 cm^3 of peat and put it into a beaker with about 100 ml of water and added a tablet of *Lychopodium* (batch nr. 177745 for Rog2 and Rog11 and batch nr. 938934 for Rog8) as a foreign substance. After this the beakers were put on a hot plate for about 15 min so that the tablets were fully dissolved. After the beakers had cooled the content was sieved through a 15 μm and a 300 μm sieve. The 300 μm sieve was put on top to remove the bigger particles and the 15 μm sieve under to let the smaller molecules, such as water through. After this, the remaining peat on top of the 15 μm sieve was collected into a test tube with the help of water and centrifuged for 5 min at 3 000 rpm. The residue on the bottom of the test tubes was then transferred into a 5 ml cup with a lid (named: core + depth, e.g., Rog2/1) and put into the fridge for storing Booth et al (2010).

The TA taxa where then identified to species or 'type' level with the help of Sullivan & Booth (2007) working draft and a light microscope with a x200 or a x400 magnification. As Payne & Mitchells (2009) article suggest a total of 100 TA individual was counted from each sample and a minimum of 50 individuals in the more degraded samples. When a minimum of 50 TA individuals could not be reached within a reasonable use of time, the counting was ended.

After the microscoping was finished the data was transferred into Excel (Microsoft, Office 365), one tab with counts and another with percentage data.

2.3.2. Radiocarbon and lead dating

The peat cores used in this thesis were dated by using two traditional methods: Radiocarbon ^{14}C and lead ^{210}Pb. These two methods where chosen because they complement each other, especially when the samples are overlapping. All samples were freeze-dried and grinded before the actual dating process was started.

The radiocarbon method is based on the radioactive isotope ^{14}C that is constantly being created in the atmosphere when cosmic radiation transforms a small number of nitrogen nuclei into radioactive nuclei of ^{14}C. Some of the radiocarbon is then taken up by plants in the form of CO_2 during photosynthesis before it is passed along in the food-chain. When the organisms eventually die the radiocarbon starts to decay (half-life: 5730±30 years) (Hine 2019). A comparison of ^{14}C levels in fossil samples to modern, enables age determination. When reporting radiocarbon ages (BP = before present), Anno Domini (AD) 1950 is used as a zero year for the chronology (Millard 2014). However, the amount of ^{14}C in the atmosphere is not constant, due to variations in the cosmic-ray bombardment

that is dependable on the solar activity (Allaby 2019). Calibration curves, which have been available since the 1960s to enable age corrections. Nowadays, there are several datasets available for the calibration, but a major part of the radiocarbon dating being published, uses one of the internationally agreed calibration curves: IntCal13, Marine13, SHCal13 and Post-bomb calibration curves NH1, NH2, NH3, SH1-2 and SH3 (Millard 2014; Blaauw & Christen 2020b).

For the radiocarbon dating 2 – 3 samples were taken from each core, one or two from the middle part and always one from the bottom of the core. A total of 8 samples were taken for ^{14}C analyses from my cores. Rog2 depth: 14, 27 and 40, Rog8 depth: 17 and 35 and Rog11 depth: 18, 33 and 48.

The chosen ^{14}C samples were sent to the Finnish museum of natural history (LUOMUS) laboratory of chronology, which operates under the University of Helsinki. There they did a so called (AAA) acid-alkali-acid treatment to the peat samples. In this method the samples are first burned to create CO_2, then the gas is gathered and converted to solid graphite by using a zinc reduction and iron-catalysed reduction (Slota et al. 1987, Palonen et al. 2013). Then the amount of radiocarbon is measured with the AMS (Accelator Mass Spectormetry)-method by using the University of Helsinki's particle accelerator (Tikkanen et al 2004). The results were given in BP ages according to Millard (2104) recommendations.

For the lead dating, samples were taken from each core every other cm starting from the top (1,3,5…etc) down to 31 cm, which makes a total of 48 samples. Overall, me and four other team members dated about 240 samples during our two weeks stay at the University of Exeter, United Kingdom in the spring 2019.

Compared to the radiocarbon ^{14}C method, which is suitable for older than 1950 AD samples, until 40 000 years (Charman, 2002). The ^{210}Pb-method is better suited for younger samples (0 – 150 years old) due to ^{210}Pb much shorter half-life (22.3 years) (Appleby 2001). The method itself has proven very reliable, especially in stable conditions, such as peat (MacKenzie et al. 1998, Vile et al. 1999). When modelling the ^{210}Pb results there are two different approaches: CRS (constant rate of ^{210}Pb supply) and CIC (constant initial concentration). Of these two, CRS is more commonly used and therefore it was also used in this project. The CRS model assumes that there is a constant supply of atmospheric ^{210}Pb being deposited and incorporated into the ground and therefore the amount of ^{210}Pb should be highest at the top of the peat column due to ^{210}Pb decay (Appleby 2001). The method itself is thus, an estimation of the residual amount of radioactivity at each sample depth (Appleby &

Oldfield 1978). ^{210}Pb itself is a naturally occurring isotope and it is part of the ^{238}U decay series (^{238}U → ^{226}Ra → ^{222}Rn → ^{210}Pb → ^{210}Po → ^{206}Pb). However, there is a disequilibrium between ^{210}Pb and its parent isotopes, due to the shift in the decay series between the ground and the atmosphere. When ^{222}Rn is being produced only a fraction of it is able to escape from the soil into the atmosphere, where it then goes through a series of short-lived radionuclides before it becomes ^{210}Pb. ^{210}Pb is then removed from the atmosphere either through wet or dry deposition before it again is incorporated to the soil (Appleby 2001).

Under the assumptions of CRS, we used a process adapted for organic material, which measures ^{209}Po decay as a proxy for ^{210}Pb by alpha spectrometry.

Each sample, of about 0.5 g of dry weight, was first put in their own labelled decanter glass and then put on a hot plate, where a 1 ml spike of ^{209}Po was added. After this the acid digestion to remove organic matter was started by adding concentrated acids (10 ml (70%) HNO_3, 10 ml (30%) H_2O_2 and 2*5 ml 6 M HCl) and letting them boil dry in between before the next one was added. After the last treatment round was completed the last step was repeated again but now the samples were left for an hour to soak. Next, the samples were transferred into centrifuge tubes and centrifuged for 10 min at 2500 rpm. The supernatant was then transferred into acid-washed jars with 0.2 g of ascorbic acid and a magnet stirrer. Before they were then topped off with about 40 ml of 0.5 M HCl. Into each jar a silver plated planchet (which was painted on the other side) was also rigged with the help of some fishing line. Finally, the jars were closed and put on a magnetic stirring table for 24 h so that as much ^{209}Po as possible would be transferred onto the silver planchet. The next day the silver planchets where rinsed under deionized water and put to dry before they would be ready for counting.

The ^{210}Po decay was measured in the University of Exeter Radiometry Laboratory. The silver planchets were put into the alpha spectrometry machine for about a week to get the highest possible count. This was, however, not possible for the deepest samples, cause their Po activity was almost zero (Estop- Aragonés et al. 2018). After all the results were ready (some samples had to be rerun), PhD candidate Sanna Piilo transferred the ^{210}Pb activities for each core into age-depth profiles based on the CRS-model by Appleby (2001) from where the real ages then could be estimated (Kelly et al. 2017).

When both the radiocarbon ^{14}C and ^{210}Pb dating was done. Age-depth models where constructed by combing the radiocarbon ^{14}C data and the ^{210}Pb data in R version 3.6.0 (R-Core- Team 2019) by using

Bacon age-modelling software (pre-R-package version 2.2), the post-bomb calibration curve NH1 and the Bacon manual – v2.3.9.1 (Blaauw & Christen 2020; 2020b).

2.3.3. Water table depth (WTD) reconstruction

Hydrological reconstructions based on TA-data and a transfer function approach is for instance used as a proxy for climate change modelling of the Holocene. A transfer function is a statistical model that apply the observed modern ecological data on modern TA training set via a range of mathematical approaches to fossil data. So that the reconstruction of the wanted environmental variable is possible (Juggins & Birks, 2011). In ombrotrophic systems the main regulating variable for TA taxa composition is hydrology, because the range for nutrient and pH variability is narrow. However, if you include systems covering the whole trophic range, the hydrological factors become less important, while the importance of nutrient availability and pH rises (Zhang et al. 2018a)

When transfer functions are dependent on the modern training sets, which is connected to a specific geographical region. Therefore, choosing a regionally valid modern training set for the reconstructions is a key for robust outcomes. As e.g., Turner et al. (2013) and Swindles et al. (2015a) stated, it is only the absolute values and magnitudes of the reconstructed WTD that may vary, while the timing and general variations of change is fairly constant, even if you used a different modern training set. Based on this assumption the Pan-European modern training set was used on my data (Amesbury et al. 2016). I also did a parallel test with another newly established modern training set created by Zhang et al. (2017), which is based solely on samples from the subarctic zone in Fennoscandia and western Russia. This comparison was done to evaluate is applying different modern training set to same data results in similar reconstruction outcome.

Data analyses and visualisation were performed in RStudio (R version 3.6.0 R-Core-Team 2019) using the packages Vegan (Oksanen et al. 2019) and Rioja (Juggins 2019). For the analysis the tolerance-downweighted averaging, with inverse deshrinking (WA-Tol (inv)) model was first run as recommended by (Amesbury et al. 2016) before the data was cross-validated with the leave-one-out method. Then the model was applied to a harmonised version of my fossil data (Table 2, Amesbury et al. 2016). The model was run with standard errors based on 1000 bootstrapping cycles. Due to the uncertainties of the exact magnitude of the reconstructed WTD values the data was also standardised using Z-scores (R Basic package) as recommended by Swindles et al. (2015a) to make the interpretation of the results more reliable. A cluster analysis according to the Bray-Curtis method was

also performed on the data. The results were visualised as a stratigraphic diagram in RStudio based on instructions provided by Matthew Amesbury. The stratigraphic diagram was based on percentage TA data with a minimum abundance of 5% to minimize the effect of rare taxa. In the diagram the reconstructed WTD in cm, the z-scores and the cluster analysis were also presented.

3. Results

3.1. Age-depth models and peat accumulation patterns

The age-depth models show at which rate the peat has accumulated over time (Figure 6). According to the age-depth models the basal age of Rog2, at 40 cm, is 6130 cal. BP, Rog8, at 35 cm, is 2820 cal. BP and Rog11, at 48 cm, is 5540 cal. BP.

Rog2. The peat accumulation rate is ca. 0.13 mm yr^{-1} for the bottom part of the core, 6060 – 5440 cal. BP. Between 5200 – 100 cal. BP the accumulation rate decreases to ca. 0.03 mm yr^{-1}, before it starts to increase again. AD 1875 – 1975 the accumulation rate is ca. 0.4 – 0.6 mm yr^{-1} and at the top of the core the accumulation rate continues to increase to ca. 2 – 2.5 mm yr^{-1}, AD 1980 – 2015. The mean peat accumulation rate for the whole core is 0.6170 mm yr^{-1}.

Rog8. The peat accumulation rate increases steadily from ca. 0.05 mm yr^{-1} at the bottom of the core to ca. 0.1 mm yr^{-1}, 2820 – 220 cal. BP. The steady increase continues and is ca. 0.3 – 0.8 mm yr^{-1} AD 1760 – 1960, ca. 1.1 – 1.7 mm yr^{-1} AD 1970 – 2000 and ca. 3.3 mm yr^{-1} at the top of the core, AD 2005 – 2015. The mean peat accumulation rate for the whole core is 0.7233 mm yr^{-1}.

Rog11. The peat accumulation rate is ca. 0.04 – 0.06 mm yr^{-1} at the bottom of the core, 5540 – 2070 cal. BP. From there it slowly starts to increase to ca. 0.1 mm yr^{-1}, 1960 – 240 cal. BP., ca. 0.2 – 0.4 mm yr^{-1} AD 1780 – 1955, ca. 1.0 – 1.7 mm yr^{-1} 1965 – 2000 before it reaches ca. 2.5 – 3.3 mm yr^{-1} at the top of the core, 2005 – 2015. The mean peat accumulation rate for the whole core is 0.4288 mm yr^{-1}.

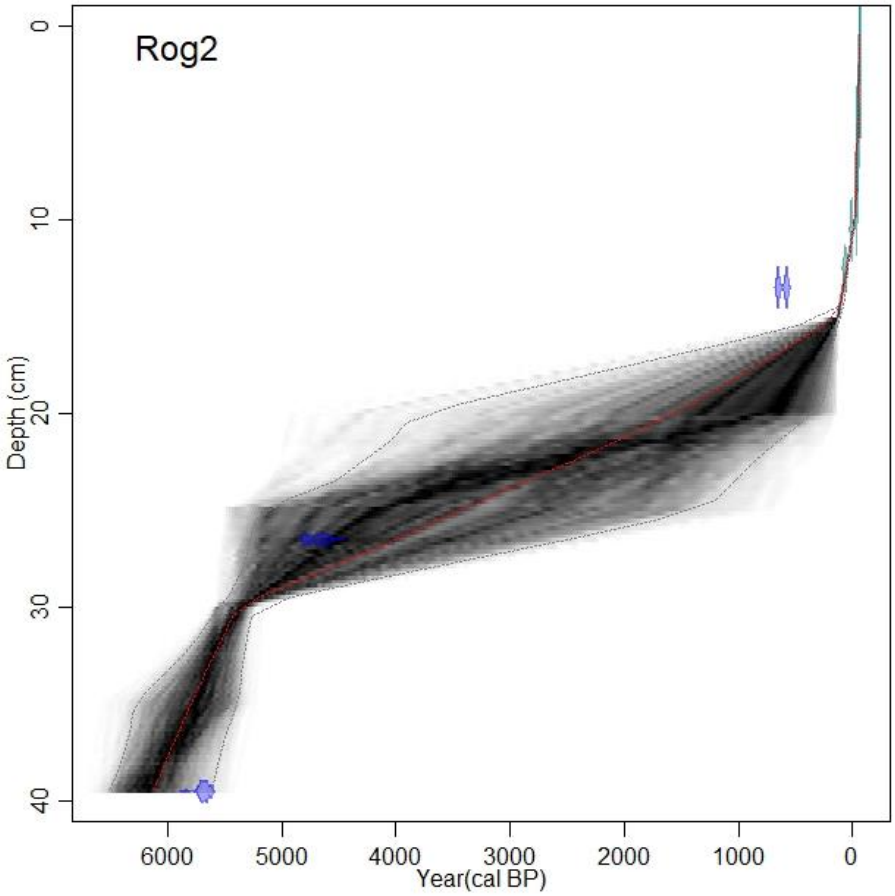
Rog2
Depth (cm)
0
10
20
30
40
6000
5000
4000
3000
2000
1000
0
Year(cal BP)

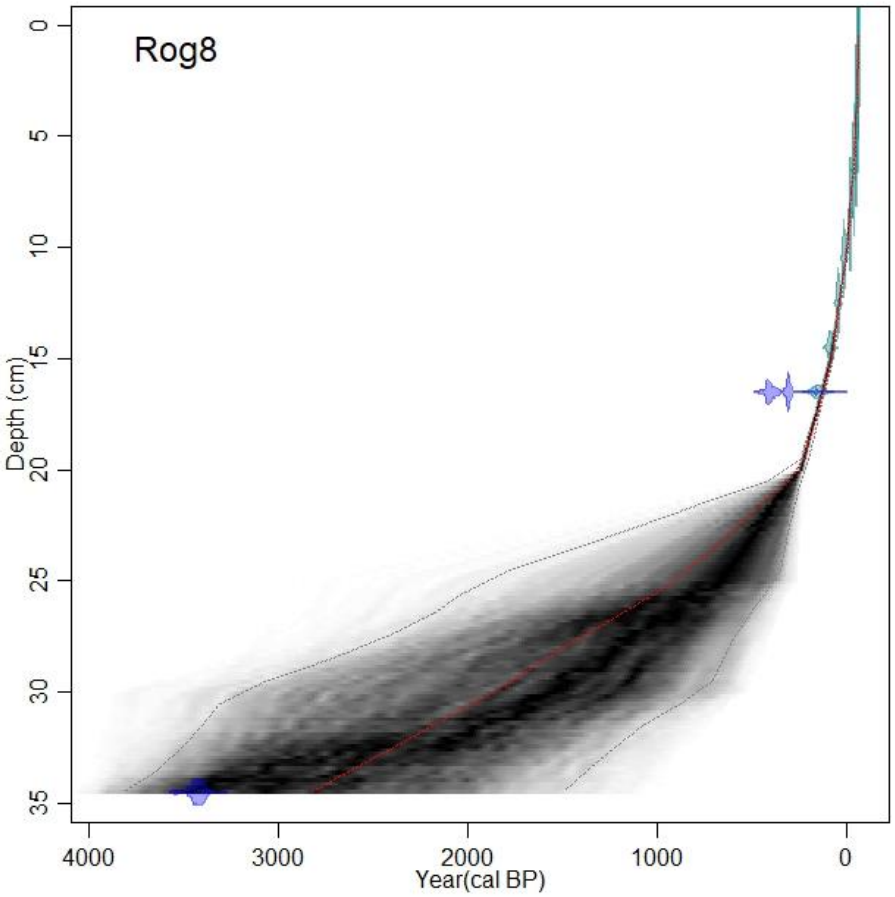
Rog8
Depth (cm)
0
5
10
15
20
25
30
35
4000
3000
2000
1000
0
Year(cal BP)

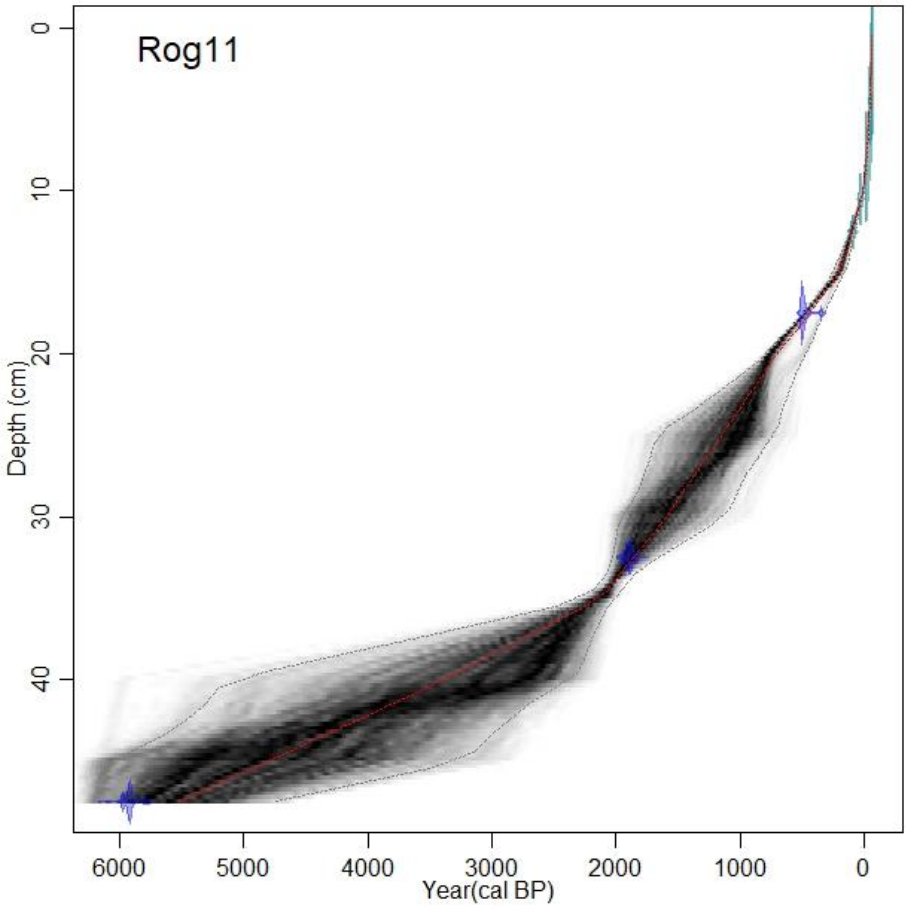

Figure 6. Age-depth models for the three cores constructed with BACON. The darker blue lines refer to the uncertainty ranges in ^{14}C, and the green blue line to uncertainty ranges in ^{210}Pb. The shaded area shows the uncertainty ranges for the age-depth model. The darker the color the more certain is the model is. The red line shows the closest fit based of the weighted mean ages of each depth (Blaauw & Christen 2020b).

3.2. Reconstructed water table depths

When discussing my reconstructed water table depth data, I have followed the niche categorization of Amesbury et al. (2016). Similarly, I also used their modern training set and transfer function procedure when processing my TA data. The WTD varies between 0 – 30 cm and the taxa can be divided into three habitat categories: wet (WTD < 10 cm), intermediate (WTD 10 – 15 cm) and dry (WTD > 15 cm). The intermediated category was further divided into two (intermediate +/-) at 15 cm because its' species richness is the highest (Table 2).

Table 2. Taxa identified for Rogovaya site. The taxa are divided into categories depending on their WTD optima based on Amesbury et al. (2016). Wet < 10 cm, Intermediate 10 – 20 cm and Dry >20 cm. The intermediated category was further divided into two subcategories 10 – 15 cm and 15 – 20 cm.

Wet	**Intermediate**		**Dry**
WTD <10cm	10 ≤ WTD ≤ 15cm	15 ≤ WTD ≤ 20cm	WTD >20cm
Archerella flavum	*Hyalosphenia papilio*	*Nebela flabellum*	*Alabasta militaris*
Placocista spinosa type	*Hyalosphenia elegans*	*Hyalosphenia subflava*	*Bullinaria indica*
Difflugia rubescens	*Heleopera petricola*	*Heleopera sylvatica*	*Trigonopyxis minuta* type
Sphenoderia lenta	*Pseudodifflugia fulva* type	*Heleopera rosea*	*Trigonopyxis arcula* type
	Difflugia pristis type	*Euglypha rotunda* type	*Nebela tincta*
	Difflugia lucida type	*Euglypha tuberculata type*	*Corythion-Trinema type*
	Phryganella acropodia	*Euglypha strigosa* type	*Assulina muscorum*
	Cyclopyxis arcelloides type	*Hyalosphenia minuta* type	
		Assulina seminulum	
		Arcella catinus type	
		Arcella artocrea	

A cluster analysis was applied to the TA data of each peat core. The analysis divided the data into four zones depicting the changes in the moisture conditions. These changes are visualised by changes in the cm-values and z-scores. The z-scores indicates the moisture trend: $z < 0$ indicating wet conditions and $z > 0$ indicating dry conditions.

Rog2. The statistical TA analysis included samples 1 – 11, because the amount of TA found in samples 13 – 40 was below 50. Samples 1 – 11 were further divided into four zones according to the cluster analysis and the borderlines of the zones are placed at 2 cm (AD ~2010), 6 cm (AD ~1995) and 8 cm (AD ~1985) (Figure 7). The age of the sample from the depth 11 cm was dated to AD ~1960.

A total of 20 taxa were found from the peat core Rog2 and throughout the core *Alabasta militaris* (dry) was the most common taxa with an abundance between 16 – 39 %. Other taxa that reached occurrences of 20 %, at least occasionally, were *Archerella flavum* (wet), *Cyclopyxis arcelloides* (intermediate -), *Euglypha strigosa* (intermediate +), *Hyalosphenia elegans* (intermediate -) and *Nebela tincta* (dry). Taxa such as *Bullinaria indica, Difflugia lucida, Difflugia rubencene, Hyalosphenia papilio, Nebela flabellulum, Phryganella acropodia* and *Trigonopyxis minuta* were excluded from the analysis because their abundance subceeded 5%.

In the first zone (AD 1960 – 1985) many taxa at least occasionally occur relatively abundant, ca. 20 %. These are *A. militaris, Archerella flavum, C. arcelloides* and *N. tincta.* Of these taxon *A. flavum*, which is more common at the bottom represents wet WTD conditions, while *N. tincta* is more abundant in the upper parts of the zone and represents dry WTD conditions. Other taxa, such as, *Difflugia pristis, Euglypha tuberculata, Pseudodifflugia fulva* and *Placosista spinosa* occur only in small numbers. These taxa mainly represent wet to intermediate WTD conditions.

In the second zone (AD 1985 – 1995) the abundance of *A. militaris* (dry) and *A. flavum* (wet) increases and they become the dominant taxa. There are also small occurrences of *E. tuberculata* (intermediate +), *N. tincta* (dry), *D. pristis* (intermediate -), *P. spinosa* (wet), *P. fulva* (intermediate -) and *Euglypha strigosa* (intermediate +). Of these, the taxa that represents dryer WTD conditions slightly decreases compared to the previous zone, except for *E. strigosa*, while the abundance of the taxa that represents wetter WTD conditions is roughly the same.

In the third zone (AD 1995 – 2011) *A. militaris* (dry) reaches its maximum abundance of ca. 35 %, while the occurrence of *A. flavum* (wet) drops to below 10 %. Of the other taxa the abundance *E. strigosa* and *Hyalosphenia elegans*, which indicates intermediate WTD conditions, increases and reaches an abundance of ca. 20 %. In this zone, there are also small occurrences of *N. tincta* and *P. spinosa.*

In the topmost zone (AD 2015) the occurrence of *A. flavum* increases compared to the previous zone, and reaches its maximum abundance of ca. 35 %, while the abundance of *A. militaris* decreases to ca. 30 %. *E. strigosa, H. elegans* and *N. tincta* all occur at an abundance of ca. 10 %. Compared to the previous zone the occurrence of the intermediate taxa *E. strigosa* and *H. elegans* decreases, while the occurrence of *N. tincta*, which represents dry conditions increases.

The values for the reconstructed WTD varies between 13 – 20 cm through the core (Figure 7). The WTD is ca. 15 cm at the bottom of the core, AD 1960. From there the WTD increases to 17 cm in AD 1980 and it becomes dryer. After this, there is a change and the moisture conditions become wetter and the WTD decreases to 14 cm in AD 1990, before it slowly increases back to dryer conditions at ca. 20 cm in AD 2007. From there the moisture conditions changes towards wetter conditions again and WTD reaches ca. 13 cm at the top of the core.

The z-scores for Rog2 follows the division of the cluster analysis well (Figure 7). In the bottom most zone (zone 1) and the third zone, where the reconstructed WTD values reaches 20 cm, which indicates dry conditions, the z-scores are positive, which also in an indication of dryer conditions. In the second and fourth zones, on the other hand, where the WTD reaches 10 cm the z-scores are negative, which also indicates towards wetter moisture conditions in the same as the high WTD values does.

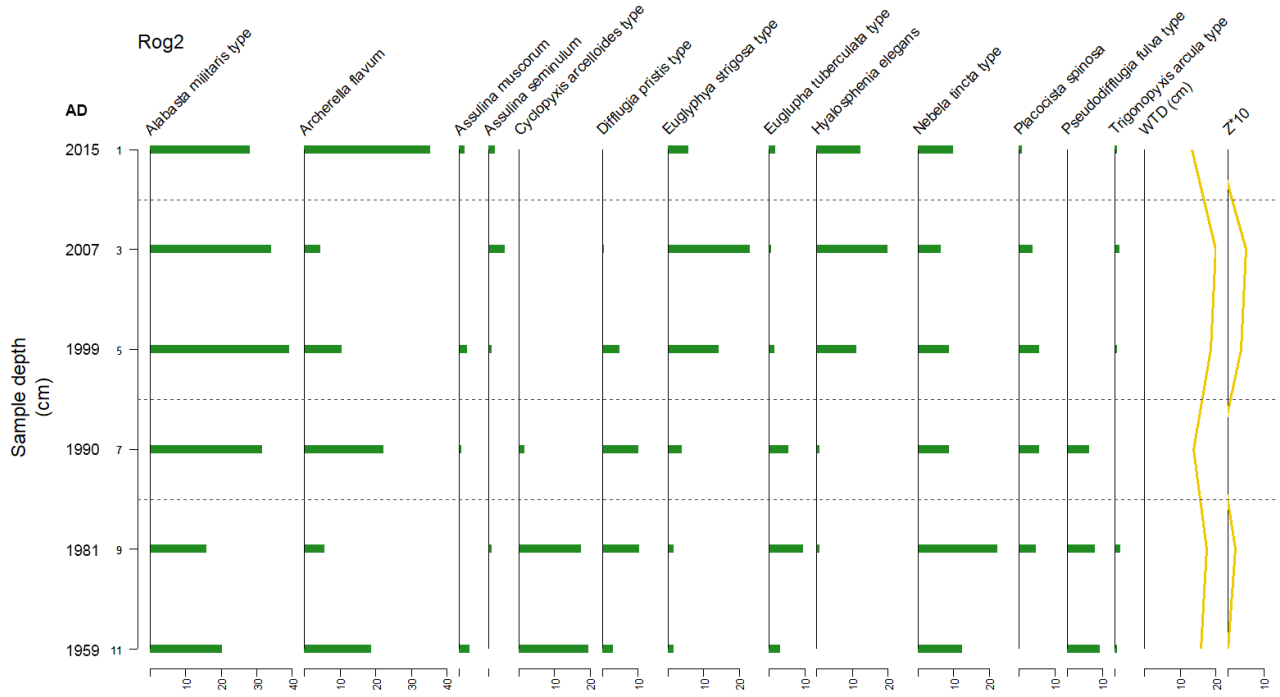

Figure 7. Percentage data of testate amoeba with an occurrence > 5 %, WTD reconstruction (cm) and Z-scores multiplied by 10 (Z < 0 indicating wet conditions, Z > 0 indicating dry conditions) plotted against the age (AD) and sample depth. The horizontal lines mark the four zones, which are based on the cluster analysis.

Rog8. The statistical TA analysis included samples 1 – 21, because the amount of TA found in samples 13 – 40 was below 50. Samples 1 – 21 were further divided into four zones according to the cluster analysis and the borderlines of the zones are placed at 8 cm (AD ~1980), 14 cm (AD ~1895) and 20 cm (AD ~1730) (Figure 8). The age of the sample from the depth 21 cm was dated to AD ~1645.

A total of 27 taxa were found from the peat core Rog8 and taxa that, at least occasionally, reached an abundance of 20 % were the wet taxa *Archerella flavum* and *Placocista spinosa*, the intermediate taxa *Hyalopshenia papilio*, *Pseudodifflugia fulva*, *Difflugia pristis*, *Difflugia lucida* and *Euglypha strigosa*

and the dry taxa *Alabasta militaris*. Other taxa that also occurred in smaller numbers were *Assulina muscorum, Assulina seminulum, Cyclopyxis arcelloides, Heleopera petricola* and *Phryganella acropodia.* Taxa such as *Arcella artocrea, A. catinus, Difflugia rubescens, Euglypha rotunda, Heleopera rosea, Hyalosphenia minuta, Hyalosphenia subflava* and *Nebela flabellum* were excluded from the analysis because their abundance subceeded 5 %.

In the first zone (AD 1645 – 1730) the intermediated - taxa *D. lucida* is the most common taxa with an abundance of ca. 25 %. The dry taxa *N. tincta* is also common with an abundance of ca. 15 %. Other taxa that also occur in this zone are the intermediate and wet taxa *A. flavum, A. seminulum, D. pristis, E. tuberculata* and *P. fulva*.

In the second zone (AD 1730 – 1895) the abundance of the wet taxa *A. flavum* increases to ca. 30 % and it becomes the most abundant taxa. Other taxa that also occur, at least occasionally, in this zone but reaches a maximum abundance of 10 – 15 % are *A. muscorum*, *N. tincta*, *A. militaris*, *D. pristis*, *E. tuberculata*, *H. papilio*, *Heleopera petricola* and *Phryganella acropodia*. These taxa mainly represent intermediate to dry WTD conditions.

In the third zone (AD 1895 – 1980) *D. pristis*, *A. militaris* and *P. fulva* are the most common taxa, representing intermediate to dry WTD conditions. *D. pristis* reaches its maximum abundance at the bottom of the zone at ca. 40 %, while *A. militaris* and *P. fulva* are more common in the upper parts of the zone reaching a maximum abundance of ca. 25 %. The taxa *A. flavum*, *C. arcelloides*, *N. tincta* and *P. spinosa* also occur through the zone but in smaller numbers.

In the topmost zone (AD 1980 – 2015) the abundance of *A. militaris* continues to increase to a maximum of 40 %, while the occurrence of *D. pristis* and *P. fulva* disappears. Taxa whose occurrence also increases are *A. flavum* (wet), *E. strigosa* (intermediate +) and *N. tincta* (dry) but only to a maximum of 15 – 25 %. The topmost cm is a bit different from the rest of the zone because the abundance of *A. flavum* and *H. papilio* (intermediate -) increases drastically to 40 respectively 20 %, while the abundance of *A. militaris* decreases to only ca. 10 % and *E. strigosa* totally disappears.

The values for the reconstructed WTD varies between 9 – 18 cm trough the core (Figure 8). The WTD is ca. 15 cm at the bottom of the core, AD 1650. From there the WTD decreases towards wetter conditions and reaches ca. 9 cm in AD 1900. After this the moisture condition changes and it becomes dryer. The WTD increases steadily until AD 1970 after which, it stabilizes and reaches its maximum

depth at ca. 18 cm in AD 2010. From there the moisture conditions changes again and it becomes wetter. This time the decrease is much faster and reaches 11 cm in AD 2015.

The z-scores for Rog8 can be seen in Figure 8. Overall, the z-scores indicates that most of the core have had moist conditions because the z-scores are below zero. However, there is a slight indication of intermediate conditions in zone 1 in AD 1650 and a little longer period with intermediate to dry conditions AD 1970 – 2010 were the z-score are slightly positive.

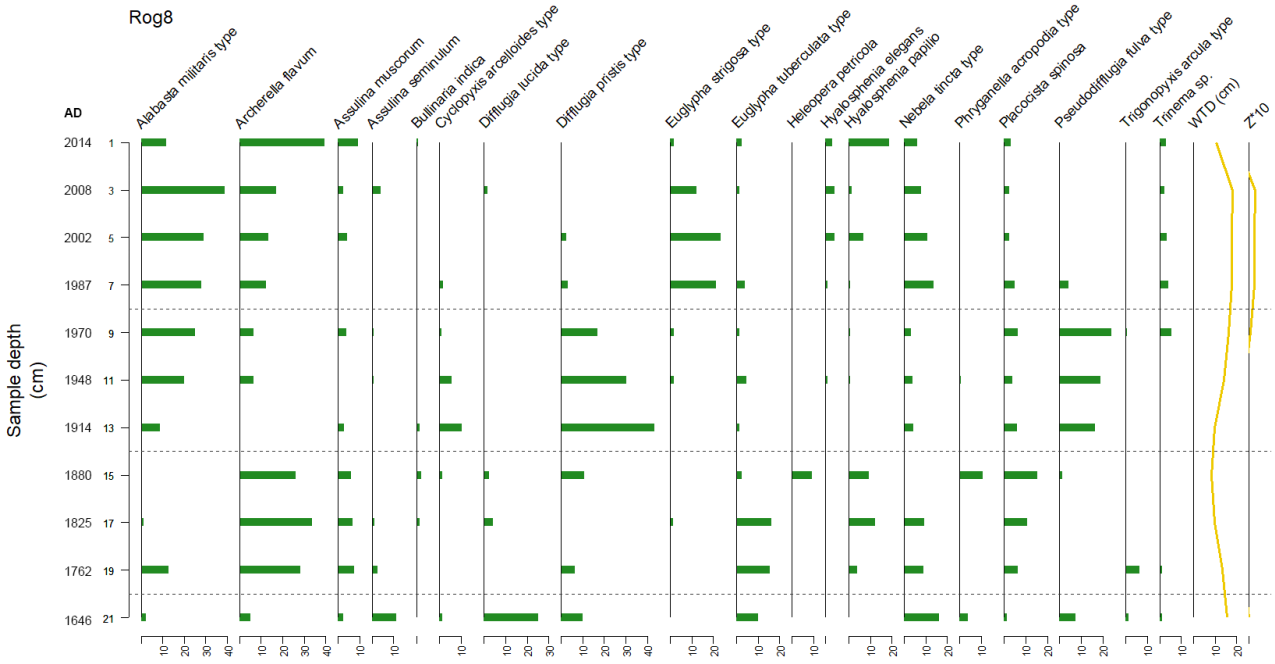

Figure 8. Percentage data of testate amoeba with an occurrence above 5 %, WTD reconstruction (cm) and Z-scores multiplied by 10 (Z < 0 indicating wet conditions, Z > 0 indicating dry conditions) plotted against the age (AD) and sample depth. The horizontal lines mark the four zones, which are based on the cluster analysis.

Rog11. The statistical TA analysis included samples 1 – 27, because the amount of TA found in samples 29 – 49 was below 50. Samples 1 – 27 were further divided into four zones according to the cluster analysis and the borderlines of the zones are placed at 10 cm (AD ~1955), 16 cm (AD ~1710) and 24 cm (AD ~940) (Figure 9). The age of the sample from the depth 27 cm was dated to AD ~670.

A total of 23 taxa was found from the peat core Rog11 and two of the most dominating taxa in the bottom half of the core are *Archerella flavum* and *Archella catinus* with an abundance that occasionally reaches over 80 %. Other taxa that reaches an abundance of 20 % or more are *Alabasta*

militaris, Cyclopyxis arcelloides, *Difflugia pristis*, *Hyalosphenia elegans*, *Nebela tincta, Phryganella acropodia* and *Trigonopyxis arcula.* Taxa such as *Difflugia lucida, Heleopera sylvatica* and *Sphenoderia lenta* were excluded from the analysis because their abundance subceeded 5 %.

In the first zone (AD 670 – 940) the dominant taxon is *A. catinus* with an abundance of over 80 % in the lower part of the zone. In the upper part of the zone the abundance of *A. catinus* decreases to ca. 40 % but the abundance of *T. arcula* increases from ca. 10 to ca. 40 %. These taxa represent intermediate to dry WTD conditions. In the upper part of the zone there are also small occurrences of the wet taxa *A. flavum* and the dry taxa *Bullinaria indica.*

In the second zone (AD 940 – 1710) the wet taxa *A. flavum* takes over and becomes the dominant taxa with an abundance that varies between ca. 60 – 90 %. There are also small occasional occurrences of *A. catinus*, *A.* flavum, B. *indica* and *P. spinosa.*

In the third zone (AD 1710 – 1955) the abundance of *A. catinus* is dominating in the lower part of the zone, ca. 50 %, while *T. arcula*, ca. 35 %, dominates the middle part and *C. arcelloides*, ca. 45 %, the upper part of the zone. These taxa represent intermediate to dry WTD conditions. Other taxa that, at least occasionally, occur at an abundance of 10 – 20 % are *A. militaris, A. flavum, D. pristis* and *P. arcopodia.*

The topmost zone (AD 1955 – 2015) is the most taxon rich zone is this core with a total of 14 different taxa, compared to the other zones that only had 4 – 9 different taxa. *A. militaris* is the most common taxa in this zone and it reaches a maximum abundance of ca. 40 %. In the lower part of the zone the abundance of *D. pristis* also rises up to 30 %, momentarily. These taxa represent intermediate to dry WTD conditions. Other taxa that, at least occasionally, occur at an abundance of 15 –20 % are *A. catinus, A. flavum, H. elegans, N. tincta* and *P. spinosa.*

The values for the reconstructed WTD varies between 5 – 30 cm trough the core (Figure 9). The WTD is ca. 30 cm at the bottom of the core, AD 670, which indicates dry conditions. The WTD stays stable until AD 850 before, the moisture conditions turn wetter and reaches ca. 5 cm in AD 1030. The WTD level is stable at ca. 5 cm until AD 1400, after which, the moisture conditions become dryer and reaches ca. 25 cm AD 1855. After this, the WTD rises and reaches a wet peak in AD 1965 at ca. 15 cm before, the WTD drops to ca. 25 cm again in AD 2000 and then rises to ca. 20 cm at the top of the core, AD 2015.

The z-scores for Rog11 can be seen in Figure 9. The z-scores are positive and indicates intermediated to dry moisture conditions in the first, third and upper half of the topmost zone, while they are negative and indicates wetter moisture conditions in the second and lower half of the topmost zone.

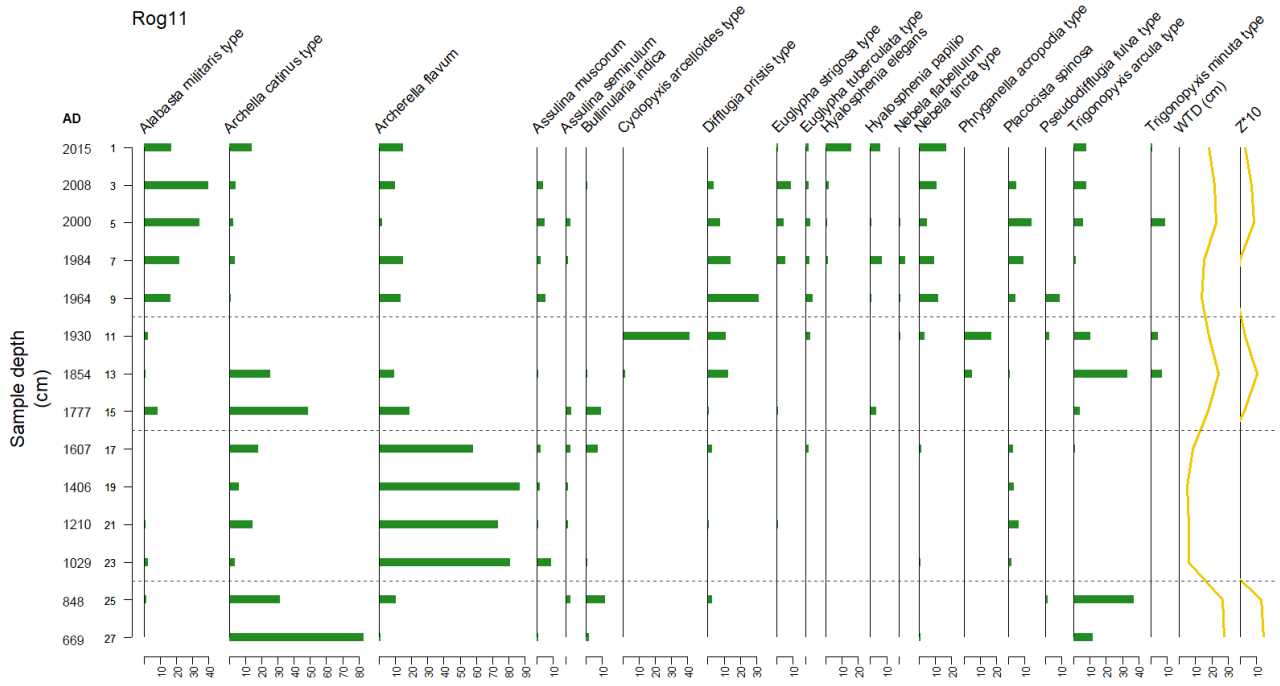

Figure 9. Percentage data of testate amoeba with an occurrence above 5 %, WTD reconstruction (cm) and Z-scores multiplied by 10 (Z < 0 indicating wet conditions, Z > 0 indicating dry conditions) plotted against the age (AD) and sample depth. The horizontal lines mark the four zones, which are based on the cluster analysis.

In total, I found 31 different taxa in the tree cores included in my thesis. Rog8 was the most taxa rich core with 27 different taxa, Rog11 was second with 23 different taxa and Rog2 last with 20 different taxa. In both Rog2 and Rog8 the dry taxa *Alabasta militaris* was the most common taxon, while the most common taxon in Rog11 was the wet taxa *Archerella flavum*.

3.3. Comparison between two WTD reconstruction outcomes based on two different modern training sets

When comparing the WTD z-scores based on two different modern training sets: Amesbury et al. 2016 (A_{tr}) and Zhang et al. 2017 (Z_{tr}), the results are quite similar (Figure 10), and this lend support for the result outcome. The p value for all cores is 0.0001128 while the R^2 value is 0.4071.

Rog2 has statistically the highest R^2 value (0.7837) and the p value is significant, 0.01899. At the bottom of the core (AD 1960) Z_{tr} z-scores start out on the negative side (wet conditions), while A_{tr} z-scores indicates intermediate conditions with a z-score near zero. From there both z-scores change towards dryer conditions and reaches the same value on the positive side (dry) in AD 1960. Between AD 1960 – 1990 the moisture conditions turn wetter, and A_{tr} z-scores reaches the negative side and wet conditions, while Z_{tr} z-scores indicates intermediate conditions near zero. After this, both z-scores indicates dryer conditions again with A_{tr} z-score rising higher than Z_{tr} in AD 2000. A_{tr} z-scores continues to rise until AD 2007 while Z_{tr} stays on the same level on the dry side. At the top of the core both z-scores turn negative (wet) with A_{tr} z-scores indicating slightly wetter conditions.

The comparison for **Rog8** is not significant with a R^2 value of 0.4214, and a p value of 0.07309. At the bottom of the core (AD 1645) the z-scores based on A_{tr} data indicates intermediate conditions near zero, while the z-scores based on the data provided by Z_{tr} indicates extremely wet conditions. From here A_{tr} z-scores slowly turn negative and reaches their lowest value in AD 1880, while Z_{tr} z-scores indicate an intermediate peak in AD 1760 before they also reach a wet peak in AD 1880. After this the z-scores based on A_{tr} data start to rise slowly and reaches intermediate conditions between AD 1950 – 1970. A_{tr} z-scores continue to rise and levels out on the positive side (dry conditions) in AD 1990 – 2010. Compared to the z-scores based on A_{tr} data do Z_{tr} z-scores rise much faster after AD 1880 and reaches their first dry peak in AD 1915. Z_{tr} z-scores then drops a bit and reaches their second dry peak in AD 1970 before they slowly turn negative and reach intermediate conditions between AD 2000 – 2010. At the top of the core, both z-scores turn negative and indicates wet moisture conditions at an equal level.

For **Rog11** the R^2 value is 0.6742 but the p value is statistically significant, 0.0003183. At the bottom of the core (AD 670) both z-scores indicate dry conditions. From there the z-scores based on Z_{tr} data have a dry peak in AD 850 before they turn negative in AD 1030, while the z-scores based on A_{tr} data indicates slightly less dry conditions in AD 850 before they become somewhat more negative in AD 1030 compared to Z_{tr} z-scores. Between AD 1030 – 1600 the z-scores for both data set indicates negative values and wet conditions with the gap between the data set staying approximately the same. Between AD 1600 – 1780 both z-scores turn positive and they both reach a dry peak in AD 1850. After this they separate and A_{tr} z-scores indicates intermediate to wet conditions in AD 1965 before they reach intermediate conditions in AD 1985, Z_{tr} s-scores on the other hand reaches a wet peak in AD 1930, a dry peak in AD 1965 and intermediate conditions in AD 1985. In the upper parts of the

core, both z-scores follow the same pattern and reaches a dry peak in AD 2000 after which the moisture conditions turn towards zero and reaches intermediate to dry conditions at the top of the core.

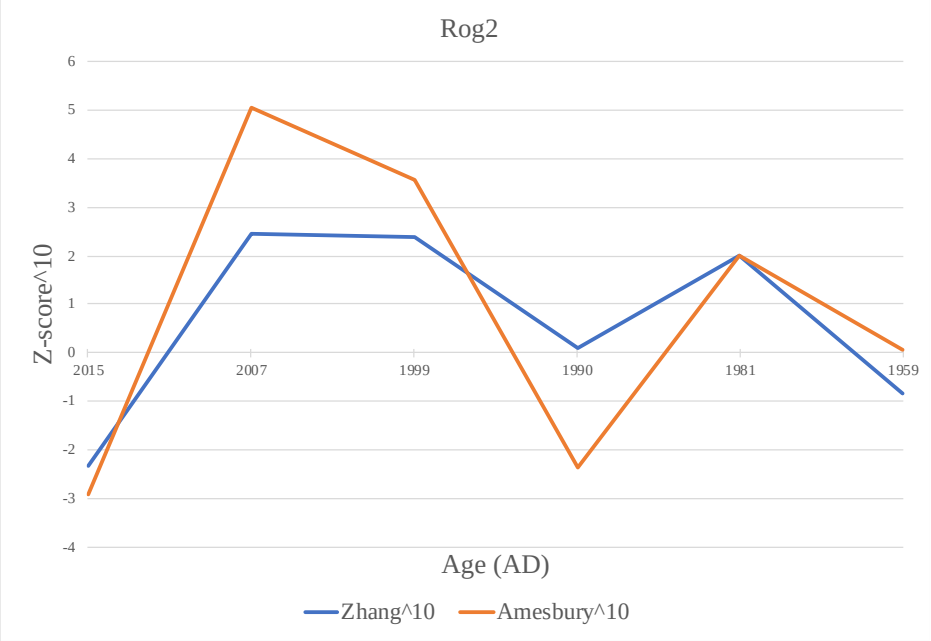

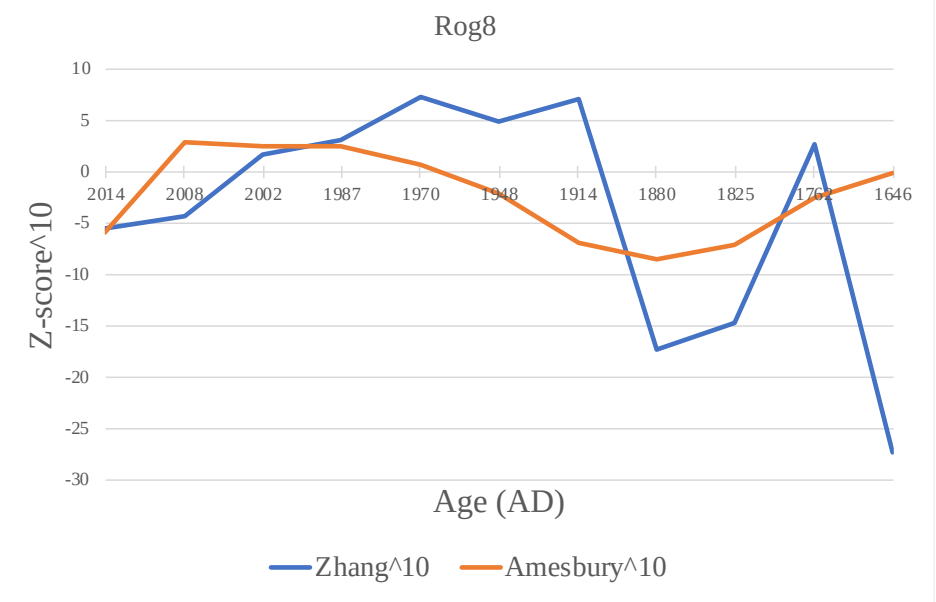

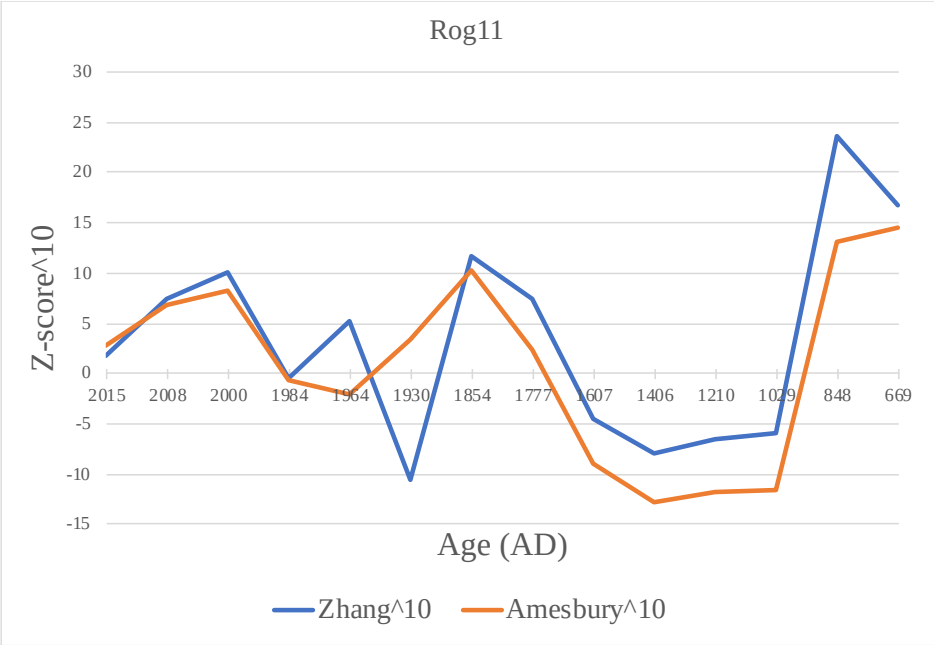

Figure 10. A z-score comparison between Amesbury et al. (2016) (red) and Zhang et al. (2017) (blue).

3.4. Carbon accumulation and plant macrofossils

The carbon accumulation and plant macrofossil analyses (Figure 11 and 12) were conducted by Mai Kärppä and Sanna Piilo, respectively, both members of the research team. The results are presented here as graphs only, to enable comparison of the testate amoebae data in the discussion.

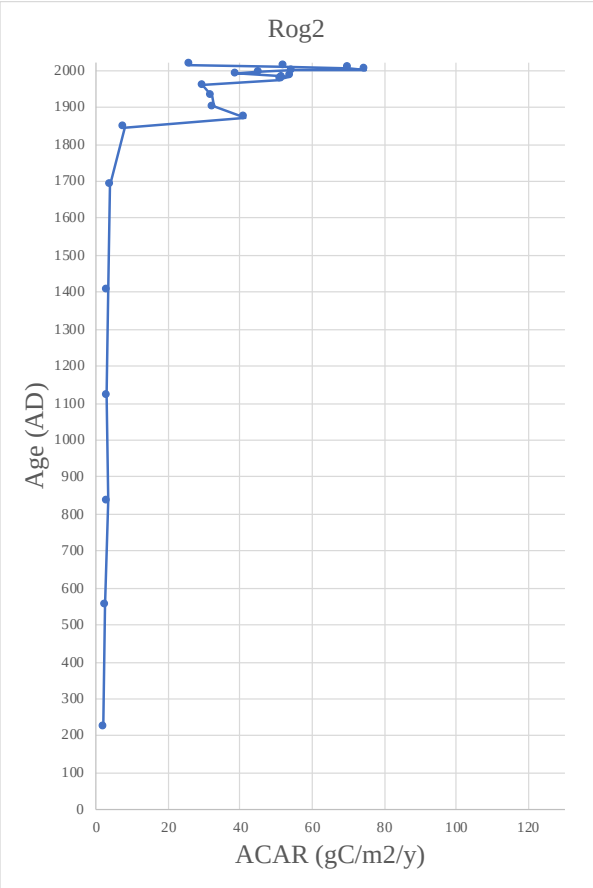

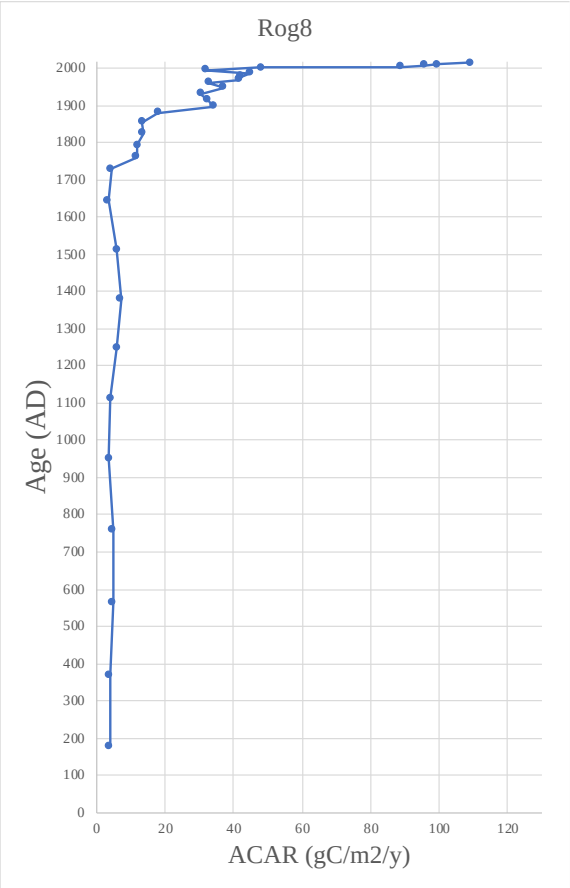

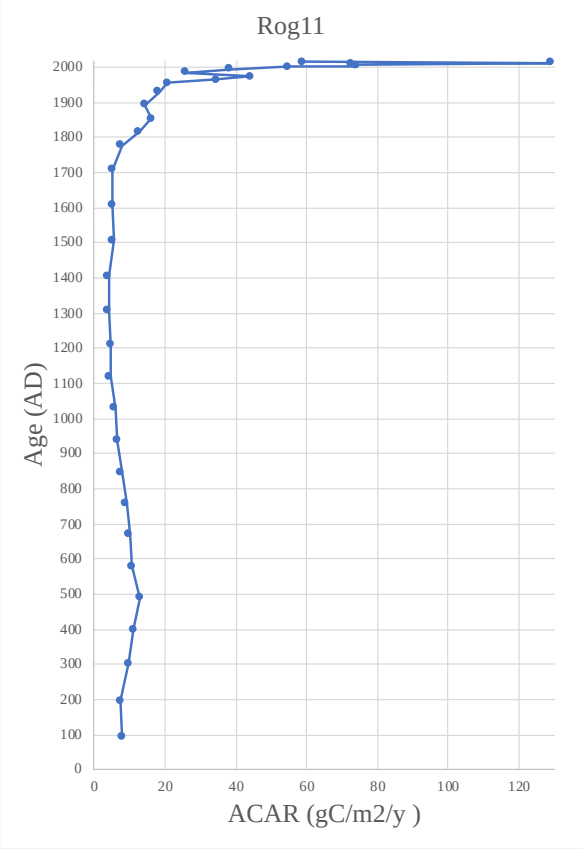

Figure 11. The apparent carbon accumulation rate ACAR (g C/m^2/y).

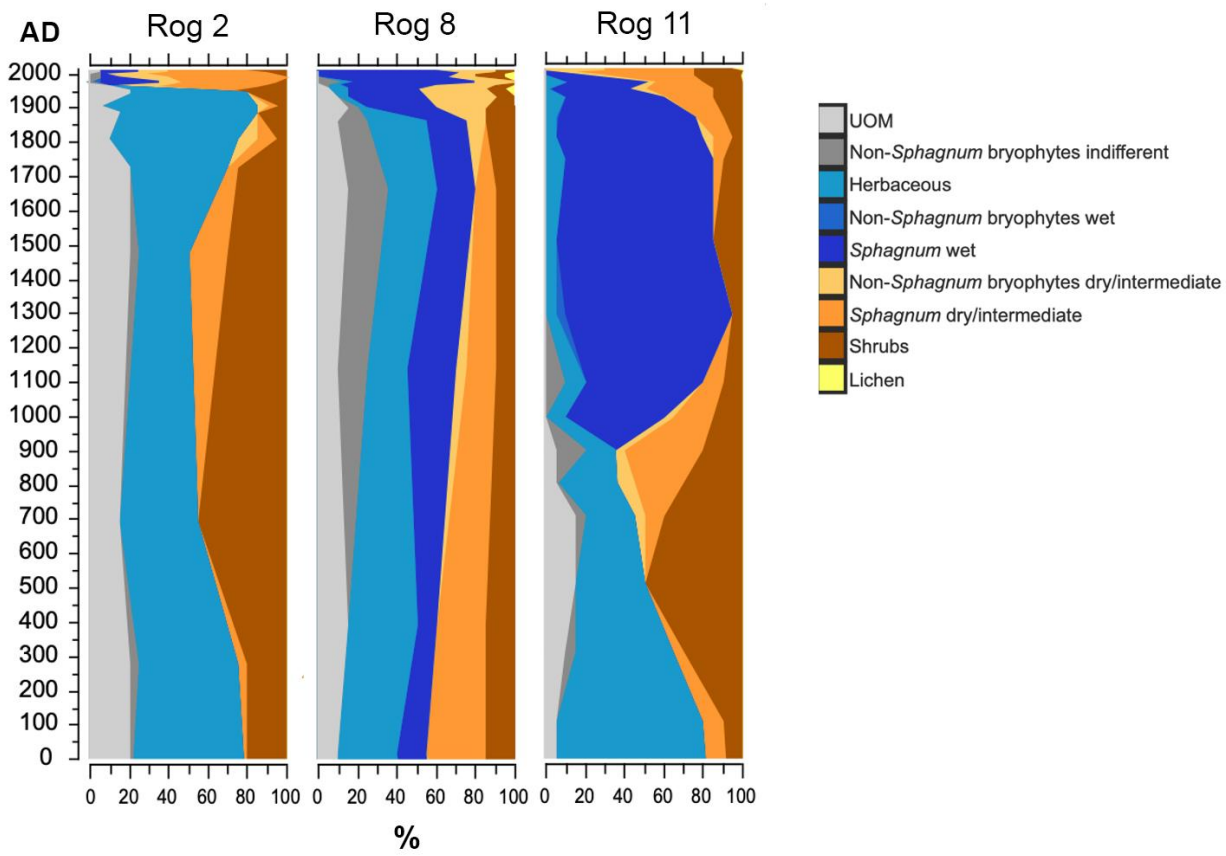

Figure 12. Plant macrofossil data in percentages, presented as plant functional types and plotted against the age in AD.

3. Discussion

3.1. Peat and carbon accumulation

Both the mean peat accumulation rate and the mean carbon accumulation rate (ACAR) for the sites in Rogovaya are comparable to other sites in northern Fennoscandia and Russia. The mean peat accumulation rate for the sites in Rogavaya was calculated as 0.6 – 1.1 mm/year compared to 0.08 – 0.67 mm/year found at the other sites and the ACAR was calculated as 22.9 – 32.4 g C m^{-2} yr^{-1}, compared to 10.8 – 32.4 g C m^{-2} yr^{-1} (Loisel et al. 2014; Treat et al. 2016; Galka et al. 2017; Sannel et al. 2018; Zhang et al. 2018b). The slightly higher values for the mean peat accumulation can be explained by me focusing my analyses on the last 2000 year and excluding older and more degraded samples.

Overall, all three cores from Rogavaya followed a similar carbon accumulation pattern during the past climatic shifts (Figure 11). They all express low ACAR values during DACP, MCA and the beginning of the LIA (ca. 3 – 7 g C m^{-2} yr^{-1}), which have also been noticed at other sites (Galka et al. 2017; Sannel et al. 2018; Zhang et al. 2018b). Apart from this, Rog11 express a small peak ca. AD 500 (ca. 13 g C m^{-2} yr^{-1}), which can be linked to an increase in shrub percentages in the plant macrofossil data during the same period (Figure 12). At the end of the LIA and beginning of the PIW the ACAR starts to rise at all sites, which is consistent with other findings (Galka et al. 2017; Sannel et al. 2018; Zhang et al. 2018b). In Rog8 and Rog11 this increasement happens gradually over a longer period of time while the change in Rog2 is more sudden. At all sites there is however a significant acceleration to the ACAR after the 1950s.

As noticed in this study and others (Galka et al. 2017; Sannel et al. 2018; Zhang et al. 2018b) there is an apparent increasement to the accumulated carbon rates towards the upper parts of the peat core. This phenomenon is, however, normal because the upper parts of the peat layers have not yet been fully decomposed (Young et al. 2019). The large amount of undecomposed peat affects the comparability of the carbon accumulation rate between older and newer layers of the peat. In an attempt to control this factor Zhang et al. 2018b have applied different models to older and newer parts of the peat, but still observed increased carbon accumulation rates for the most recent decades. Zhang et al. 2018b's observation combined with similar observations of increased carbon accumulation rates and rising temperatures could suggest that at least some of the increase in the carbon accumulation rate can be explained by changing climate conditions i.e., warming.

3.2. A proxy comparison of the hydrological conditions during the different climate periods

When comparing the data provided by the TA community to the plant macrofossils it is noticeable that they complement each other relatively well. Of the three Rogovaya cores, Rog11 provided the oldest TA data covering the end of DACP (Figure 9). Based on the reconstructed WTD provided by the TA data and the presence of *Archella catinus* and *Trigonopyxis arcula*, indicate dry conditions during this period. This signal is noticeable in the plant macrofossil data as well, where a higher amount of shrubs and dry to intermediate *Sphagnum* species is found, compared to the beginning of DACP (Figure 12). The trend of drying can also be seen in the Rog2, but not in Rog8. These finding are supported by other studies from the area, which suggest that the dryer conditions are due to permafrost aggradation and uplifted peat surfaces (Routh et al. 2014).

At the beginning of the MCA when climate conditions turned warmer, there is a strong shift from dry to wet moisture conditions at the site of Rog11 ca. AD 850 – 1050 in the TA data (Figure 9). The dry/wet transition can also be noticed in the plant macrofossil data for Rog11, but it started slightly later ca. AD 950 (Figure 12). This noticeable change to the moisture conditions is represented by the initiation of wet *Sphagnum* species in the plant macrofossil data and the occurrence of *Archerella flavum* in the TA data, which both becomes the dominating taxonomic group. The plant macrofossil data for the other cores continue to show quite stable conditions even though the amount of wet *Sphagnum* species slightly increases towards the end of the MCA in Rog8, as does the amount of dry to intermediate *Sphagnum* species in Rog2. The prominent changes to the taxa compositions at the site of Rog11, compared to the stable conditions at the other sites, indicates that the MCA-induced warming potentially resulted in a partial thaw of the permafrost, which also appeared to have happen at other sites in the NE Russia (Routh et al. 2014; Zhang et al. 2018c)

During the beginning of the LIA both the TA and the plant macrofossil data for Rog11 continues to indicate wet moisture conditions, however, a general trend of drying is also noticeable (Figure 9 & 12). In the TA dataset, the change towards dryer conditions is seen as a taxa transition from the wet taxa *Archerella flavum* to the intermediate taxa *Archella catinus* and then again to the dry taxa *Triginipyxis arcula*, while the same trend is expressed in the plant macrofossil dataset by an increasing amount of dry to intermediate *Sphagnum* species and shrubs towards the end of the LIA. However, at the same time, at site of Rog8, the taxonomic composition indicates a moisture trend towards opposite direction. The TA taxa composition changes there from including the dry taxa *Nebela tincta* to domination of wet taxa *Archerella flavum*, while there is a slight increase to the occurrence of herbaceous plants in the plant macrofossil data (Figure 8 & 12). Based solely on the plant macrofossil dataset, the same trend of wetter moisture conditions, towards the end of the LIA, also occurred at Rog2 (Figure 12). Other studies have found equal indications of dry/drying conditions due to permafrost aggradation during the beginning of the LIA as the TA dataset for Rog11 suggests (Oksanen et al. 2001; Zhang et al. 2018c). The study by Zhang et al. 2018c, however, also found indications of wetter periods towards the end of the LIA, which is similar to fluctuations found in Rog2 and Rog8.

After the transition over to the PIW the dry taxa *Alabasta militaris* becomes the dominating taxa in all cores, indicating a trend of drying-up (Figures 7 – 9). This drying can also be seen in plant macrofossil data for Rog2 and Rog11 and is supported by other findings in Fennoscandia (Galka et al. 2017; Zhang et a. 2018c; Sim et al. 2021). However, the macrofossil dataset for Rog8 show

continued indications of wetter conditions during the PIW, but there is a taxa transition from wet *Sphagnum* species to herbaceous plants. The contradiction between the two proxies, especially at the site of Rog8 might be because TA are more sensitive to environmental changes than plant communities (Väliranta et al. 2012). This fact could also explain why the wetter moisture conditions at the surface of the peat core shown in the TA datasets are not yet visible in the datasets provided by the plant macrofossil community (Figures 7 –9, 12).

3.3. Evaluation of the microscoping process and training set comparison between Amesbury's and Zhang's – sources of error

As I was not familiar with testate amoeba before I started working on this thesis some errors might have occurred during the microscoping process before I learned to recognize each taxa from the other. During the learning process I got valuable help with the identification from my second supervisor M. Amesbury and Hui Zhang. During the microscoping a smaller version of *Placocista spinosa* was found in numerous samples. The average length of these individuals where about 62.5 – 90 μm, compared to normal size 105 – 145 μm (Siemensma 2020). As TA are characterized by a high degree of morphological variability both among and within populations it is not unusual to find smaller specimens. But it is also noticeable that TA traits, such as size, can be affected by both abiotic and biotic environmental factors, such as, food source, temperature or insecticides (Mitchell et al. 2008). In this case a lower temperature could explain the variation in the size of *Placocista spinosa* as the samples were gathered from a peatland bog on the Arctic tundra.

The results of the reconstructed WTD patterns based on different modern training sets are mostly comparable. However, one of the main reasons behind the differences between the two WTD outputs is that each training set owes specific WTD optima defined for the taxa in question. In A_{tr} the largest category was the intermediate (10 – 20 cm) and therefore it was divided into two subcategories 10 – 15 cm and 15 – 20 cm. When applying the same categorization but focusing on WTD optima measured by Z_{tr} then the intermediate category, as a whole, is still the biggest while both the dry and wet category have gained more representatives. In most cases, where a taxa have two different WTD optimum according to the training sets they are in neighboring categories (Table 3). But in the cases of *Nebela tincta*, *Euglypha rotunda* and *Heleopera sylvatica* there is a gap between the two optima. *N tincta* represents the dry category based on A_{tr} the intermediate- category based on Z_{tr}, while *E. rotunda* and *H. sylvatica* represent the intermediate + category based on A_{tr} and the wet category

based on Z_{tr}. Some of the difference to the categorization could be explained by A_{tr} being based on samples from the temperate and boreal zone all over Europe, while Z_{tr} samples were collected from the subarctic tundra in the Finnish Lapland and arctic tundra in European Russia. In the Arctic and sub-arctic regions from where Z_{tr} was taken environmental conditions, such as, seasonal freezing, active-layer thickness and bare peat feature differs. However, it is also important to notice that many taxa have a relatively similar position on the WTD gradient, which suggests that hydrological factors are reflected in TA assemblages similarly and that most taxa have been able to adapt also to cooler climate conditions as well (Zhang et al. 2017). This comparison confirms that either modern training set could potentially be used to gain valid results. However, as the sample size for A_{tr} is much larger the results based on this modern training should be more robust.

Table 3. Water table depth categorization comparison between Amesbury et al. (2016) and Zhang et al. (2017).

Taxa	Amesbury	Zhang
Arcerella flavum	W	I-
Hyalosphenia papilio	I-	W
Pseudodifflugia fulva	I-	I+
Difflugia pristis	I-	I+
Difflugia lucida	I-	W
Phryganella acropodia	I-	W
Heleopera sylvatica	I+	W
Assulina seminulum	I+	D
Euglypha tuberculata	I+	D
Hyalosphenia minuta	I+	D
Euglypha tuberculata	I+	W
Alabasta militaris	D	I-
Nebela tincta	D	I+

A small sample size is also a factor that should be considered when analyzing my results, as the development of the peatlands vary. Thus, limiting the generalization of the results to a relatively small area surrounding the coring site. To be able to differentiate the autogenic factors from the allogenic, multiple samples are needed. However, as the scope of the master's thesis is limited, in-depth analyses of multiple cores is not possible. But, as this thesis is part of a larger research project, additional cores will be analyzed to provide more reliable results.

Other possible sources of error could be connected to the age-depth analysis. Despite all precautions, during the collection and analyzing phases, the peat might still be contaminated with modern carbon,

which affects the ^{14}C dating. As the sample ages always are estimates based on weighted mean ages and the error ranges are large the uncertainties remain. However, there are no inconsistencies visible in the data, which indicates that the peat layers have not been mixed by either the research team or natural causes, such as, plant root penetration or cryoturbation. In addition, a second dating method was applied in parallel, which makes the chronologies more robust.

3.4. Anwsering the hypotheses

My first hypothesis: Past climate phases are recorded in the peat as changes in the moisture conditions, cannot clearly be confirmed by my samples. In both Rog2 and Rog8 there are no distinct changes to the TA or plant macrofossil taxa compositions, which are parallel with the transition phase of climatic periods, until the end of the LIA. Rog11, on the other hand, expresses a clear wet shift during the DACP/MCA shift and a trend of drying during the LIA. However, the beginningof the 1900s is reflected in all cores as a regime shift.

My second hypothesis: Past changes in moisture conditions are reflected in testate amoeba community shifts, can be confirmed by the data by comparing the plant macrofossil data to the TA data. By doing this, it is noticeable that, especially in the case of Rog11, the taxa composition of TA changes according to the moisture changes indicated by the plant macrofossil data. And that even though, when I compared the estimated WTD level of two different training sets, the result where statistically valid.

My third hypothesis: Fossil testate amoeba assemblage can provide quantitative estimates of past peatland water table changes, is confirmed. This method is valid because changes in moisture show as changes in the taxa composition of the TA. And even though these changes do not align with climate periods shift it does not mean that the method is invalid but instead that the effect of the climate shift might have been weak in this area, which strengthens local biotic and abiotic factors of each of coring points. Compared to plant macro fossils TA are also shown to be more sensitive, which also might be an advantage, especially when studying the most recent moisture shift during the PIW.

4. Conclusions

By using testate amoeba as a proxy for moisture change in combination with dated peat samples, I was able to reconstruct past moisture shifts at the coring site in Rogovaya, Russia. The results from

the reconstruction show similar fluctuations as have been noticed in other studies nearby and some of these fluctuations can be can be connected to past climatic shifts, especially at the site of Rog11. However, as the other records do not show similar fluctuations it can be suggested that autogenic factors can have a bigger impact on both moisture conditions and carbon dynamics than climate change.

During the resent warming the general response for the northern peatlands seem to have been a trend of widespread drying and increased carbon accumulation, which also can be seen at Rogovaya. However, based on the testate amoeba data, a shift towards wetter conditions have happened during the last decade. As this shift is not yet detectable in the plant macrofossil data, is it still uncertain if the wet phase will be big enough to cause major changes to the ecosystem. However, this might still be an indication that the peatland in Rogovaya have reached its threshold between melting permafrost and the drying effect of evapotranspiration. As, these are only speculations, is the future development of the peatland's hydrology and carbon dynamics in Rogovaya still uncertain.

To conclude, my results indicates that the dynamics of both hydrology and carbon are complicated processes affected by both autogenic and allogenic factors, therefore causing large variability even on a local scale. These variations have also been noticed in other studies, which highlights the importance of a large enough number of samples, when studying the internal dynamic of peatlands. The absence of widely spread observations of the most recent wet shift also indicates that the future responses to the anthropogenic climate change might not be equal and synchronous. This complicates the estimations of how peatlands will develop in the future in response to the most recent climate change. To rectify this situation, is continued research crucial, so that we can increase our understanding of climate-peatland interactions.

5. Acknowledgements

I like to thank Dr Minna Väliranta for all the support, patience and help with the literature and structure of the thesis, and Dr. Matthew Amesbury and Dr. Hui Zhang for their help with the testate amoeba analysis and methodology. I also like to thank Sanna Piilo for allowing me to use some of her pictures, the plant macrofossil analysis and helping me with the age depth analysis. In addition, I like to extend a special thanks to Dr. Tarmo Virtanen for helping me with the maps and allowing me to use some of his pictures and Sonja Still for lending me her expertise in editing. Finally, I like to

thank the other members of the research team for the field work, dating of the peat samples and other laboratory work.

6. References

Aaby B. (1976) Cyclic climatic variations in climate over the past 5,500 yr reflected in raised bogs. Nature. 263: 281 – 284.

Alexandrov G. A., Brovkin V. A., Kleinen T. & Yu Z. (2020) The capacity of northern peatlands for long-term carbon sequestration. Biogeoscience 17: 47 – 54.

Allaby M. (Edi.) (2019) Radiocarbon dating (^{14}C dating). A Dictionary of Plant Science (4 ed.). Oxford University Press.

Alm J., Schulman L., Walden J., Nykänen H., Martikainen P. J. & Silvola J. (1999) Carbon balance of a boreal bog during a year with an exceptionally dry summer. Ecology 80: 161 – 174.

Amesbury M. J., Swindles G. T., Bobrov A, Charman D. J., Holden J., Lamentowicz M., Mallon G., Mazei Y., Mitchell E. A. D., Payne R. J., Roland T. P., Trurner T. E. & Warner B. G. (2016) Development of a new pan-European testate amoeba transfer function for reconstructing peatland palaeohydrology. Quaternary Science Reviews. 152: 132 – 151.

Appleby P. G. (2001) Chronostratigraphic techniques in recent sediments. In: Last W. M. & Smol J. P. (Eds.). Tracking Environmental Change Using Lake Sediments Volume 1: Basin Analysis, Coring and Chronological techniques. Klower Academic Publisher, Dordrecht. pp: 171 – 203.

Appleby P. G. & Oldfield F. (1978) The calculation of lead-210 dates assuming a constant rate of supply of unsupported 210Pb to the sediment. Catena. 5: 1 – 8.

Beyens L. (1985) On the subboreal climate of the Belgian campine as deduced from diatom and testate amoebae analyses. Review of Palaeobotany and Palynology. 46: 9 – 31.

Birks H. J. B. (1995) Quantitative palaeoecological reconstructions. In: Maddy D. & Brew J. S. (eds.) Statistical modelling of Quaternary science data. Technical Guide 5. Quaternary Research Association. Cambridge. 161 – 254.

Booth R.K., Lamentowicz M. & Charman D.J. (2010) Preparation and analysis of testate amoebae in peatland palaeoenvironmental studies. Mires and peat. 7: 1 – 7.

Blaauw M. & Christen A. (Cited: 2.1.2020) Bacon age-modelling software. Webpage: http://chrono.qub.ac.uk/blaauw/bacon.html

Blaauw M. & Christen A. (Cited: 6.4.2020b) Bacon manual – v2.3.9.1 Webpage: https://chrono.qub.ac.uk/blaauw/manualBacon_2.3.pdf

Brown J., Ferrians Jr O. J., Heginbottom J. A. & Melnikov E. S. (1998). Revised February 2001. Circum-Arctic map of permafrost and ground-ice conditions. Boulder, CO: National Snow and Ice Data Center. Digital media.

Camill P., Barry A., Williams E., Andressi C., Limmer J. & Solick D. (2009) Climate-vegetation-fire interactions and their impact on long-term carbon dynamics in a boreal peatland landscape in northern Manitoba, Canada. Journal of Geophysical Research. 11: G04017.

Charman D. J., Hendon D. & Woodland W. A. (2000) The identification of testate amoebae (protozoa: rhizopoda) in peats. QRA Technical guide No. 9. Quaternary Reasearch Association London. 147 pp.

Charman D. (2002) Peatlands and Environmental change. John Wiley & Sons Ltd. England. p. 8, 122 & 164 – 168.

Charman D. J., Blundell A. & Acrotelm Members (2007) A new European testate amoebae transfer function for palaeohyrological reconstruction on ombrotrophic peatlands. Journal or Quaternary Science. 22: 209 – 221.

Charman D. J., Beilman D. W., Blaauw M., Booth R. K., Brewer S., Chambers F. M., Christen J. A., Gallego-Sala A., Harrison S. P., Hugher P. D. M., Jackson S. T., Korhola A., Mauquoy D., Mitchell F. J. G., Prentice I. C., van der Linden M., De Vleeschouwer F., Yu Z., Alm J., Bauer I. E., Corish Y. M. C., Garneau M., Hohl V., Huang Y., Karofeld E., Le Roux G., Loisel J., Moschen R., Nichols J. E., Nieminen T. M., MacDonald G. M., Phadtare N. R., Rausch N., Sillasoo Ü., Swindle G. T., Tuittila E-S. Ukonmaanaho L., Väliranta M., van Bellen S., van Geel B., Vitt D. H. & Zhao Y. (2013) Climate-related chnages in peatland carbon accumulation durong the last millennium. Biogesciences. 10: 929 – 944.

Estop-Aragonés C., Cooper M. D. A., Fisher J. P., Thierry A., Garnett M. H., Charman D. J., Murton J. B., Phoenix G. K., Treharne R., Sanderson N. K., Burn C. R., Kokelj S. V., Wolfe S. A., Lewkowicz A. G., Williams M. & Hartley I. P. (2018) Limited release of previously-frozen C and increased new peat formation after thaw in permafrost peatlands. Soil Biology and Chemistry. 118: 115 – 129.

Galka M., Szal M., Watson E. J., Gallego-Ala A., Amesbury M. J., Charman D. J., Roland T. P., Turner T. E. & Swindles G. T. (2017) Vegetation succession, carbon accumulation and hydrological change in subarctic peatland, Abisko, northern Sweden. Permafrost and periglacial processes. 28: 589 – 604.

Gallego-Sala A. V., Charman D. J., Brewer S., Page S. E., Prentice I. C., Friedlingstein P., Moreton S., Amesbury M. J., Beilman D. W., Björck S., Blyakharchuk T., Bochicchio C., Booth R. K., Bunbury J., Camill P., Carless D., Chimner R. A., Clifford M., Cressey E., Courtney-Mustaphi C., De Vleeschouwer F., de Jong R., Fialkiewicz-Koziel B., Finkelstein S. A., Garneau M., Githumbi E., Hribjlan J., Holmquist J., Hughes P. D. M., Jones C., Jones M. C., Karofeld E., Klein E. S., Kokfelt U., Korhola A., Lacourse T., Le Roux G., Lamentowicz M., Large D. Lavoie M., Loisel J., Mackay H., MacDonald G. M., Makila M., Magnan G., Marchant R., Marcisz K., Cortizas A. M., Massa C., Mathijssen P., Mauquoy D., Mighall T., Mitchell F. J.G., Moss P., Nichols J., Oksanen P. O., Orme L., Packalen M. S., Robinson S., Roland T. P., Sanderson N. K., Sannel A. B. K., Silva-Sánchez N., Steinberg N., Swindles G. T., Turner T. E., Uglow J., Väliranta M., van Bellen S., van der Linden M., van Geel B., Wang G., Yu Z., Zaragoza-Castells J. & Zhao Y. (2018) Latitudinal limits to the predicted increase of the peatland carbon sink with warming. Nature Climate Change. 8: 907 – 913.

Heiskanen L., Tuovinen J-P., Räsänen A., Virtanen T., Juutinen S., Lohila A., Penttilä., Linkosalmi M., Mikola J., Laurila T. & Aurela M. (2021) Carbon dioxode and methane exchange of a patterned subarctic fen during two contrasting growing seasons. Biogeoscience 18: 873 – 896.

Hine R (Edi.) (2019) Carbon dating (radiocarbon dating). A Dictionary of Biology (8ed). Oxford University Press.

Hugelius G., Loisel J., Chadburn S., Jackson R. B., Jones M., MacDonald G., Marushchak M., Oledeldt D., Packalen M., Siewert M. B., Treat C., Turetsky M., Voight C. & Yu Z. (2020) Large stock of peatland carbon and nitrogen are vulnerable to permafrost thaw. PNAS 117: 20428 – 20446.

IPCC [Core Writing team: Pachauri R. K. & Meyer L. A. (eds.)]. (2014) Climate Change 2014: Synthesis Report. Contributing of Working Groups I, II, and III to the Fifth Assessment Report of the Intergovernmental Panel on Climate Change. IPCC, Geneva, Switzerland, 151 pp.

IPCC [Masson-Delmotte V., Zhai P., Pörtner H-O., Roberts D., Skea J., Shukla P. R., Pirani A., Mpufouma-Okia W., Péan C., Pidcock R., Connors S., Matthews J. B. R., Chen Y., Zhou X., Gomis M. I., Lonnoy E., Maycock T., Tignor M. & Waterfield T. (2018) Summary for Policymakers: In: Global Warming of 1.5°C. An IPCC Special Report on the impacts of global warming of 1.5°C above pre-industrial levels and related global greenhouse gas emissions pathways, in the context of strengthening the global response

to the threat of climate change, sustainable development, and efforts to eradicate poverty. World Meteorological Organization, Geneva, Switzerland, 32 pp.

Juggins S. & Birks H. J. B. (2011) Quantitive environmental reconstructions from biological data. In: Birks H. J. B., Lotter A. F., Juggins S. & Smol J. P. (Eds.) Tracking Environmental Change Using Lake Sediments. Springer. Netherlands, Dordrecht. pp. 441 – 494.

Juggins S. (2019) Rioja: Analysis of Quaternary Science Data. R Package Version: 0.9-2.1. Webpage: https://cran.r-project.org/web/packages/rioja/rioja.pdf.

Kelly T. J., Lawson I. T., Roucoux K. H., Baker T. R., Jones T. D. & Sanderson N. K. (2017) The vegetation history of an Amazonian domed peatland. Palaeogeography, Palaeoclimatology, Palaeoecology. 468: 126 – 141.

Kokkonen N. A. K., Laine A. M., Laine J., Vasander H., Kurki K., Gong J. & Tuittila E-S. (2019) Responses of peatland vegetation to 15-year water level drawdown as mediated by fertility level. Journal of Vegetation Science. 30: 1206 – 1216.

Lagarec D. (1982) Cryogenetic mounds as indicators of permafrost conditions, northern Quebec. 4th Canadian permafrost conference. 43 – 48.

Laine J. & Vasander H. (1996) Ecology and vegetation gradients of peatlands. In: Vasander H. (ed.) Peatlands in Finland. Finnish Peatland Society. Helsinki. 10 – 19.

Lamentowicz M., Cedro A., Galka M., Goslar T., Miotk-Szpiganowicz G., Mitchell E. D. A. & Pawlyta J. (2008) Last millennium palaeoenvironmental changes from a Baltic bog (Poland) inferred from stable isotopes, pollen, plant macrofossils and testate amoebae. Palaeogeography, Palaeoclimatology, Palaeoecology. 265: 93 – 106.

Ljungqvist F. C. (2010) A new reconstruction of temperature variability in the extra-tropical Northern Hemisphere during the last two millennia. Geografiska Annaler: Series A. 92: 339 – 351.

Loisel J., Yu Z., Beilman D. W., Camill P., Alm J., Amesbury M. J., Anderson D., Andersson S., Bochiccho C., Barber K., Belyea L. R., Bunbury J., Chambers F. M., Charman D. J., de Vleeschouwer F., Fialkiewicz-Koziel B., Finkelstein S. A., Galka M., Garneau M., Hammarlund D., Hinchcliffe W., Holmquist J., Hughes P., Jones M. C., Klein E. S., Korhola A., Kuhry P., Lamarre A., Lamentowicz M., Large D., Lavoie M., MacDonlad G., Magnan G., Mäkilä M., Mallon G., Mathijssen P., Mauquoy D., McCarroll J., Moore T., Nichols J., O'Reilly B., Oksanen P., Packalen M., Peteet D., Richard P. J. H., Robinson S., Ronkainen T., Rundgren M., Sannel A. B. K., Tarnocao C., Thom T., Tuittila E-S., Turetsky M., Väliranta M., van der Linden M., van Geel B., Vitt D., Zhao

Y. & Zhou W. (2014) A database and synthesis of northern peatland soil properties and Holocene carbon and nitrogen accumulation. The Holocene. 24: 1028 – 1042.

Luoto M., Fronzek S. & Zuidhoff F. S. (2004) Spatial modelling of palsa mires in relation to climate in northern Europe. Earth Surface Processes and landforms 29: 1373 – 1387.

MacKenzie A. B., Logan E. M., Cook G.T. & Pulford I. D. (1998) Distributions, inventories and isotopic composition of lead in ^{210}Pb-dated cores from contrasting biogeochemical environments: Implications for lead mobility. The Science of the Total Environment. 223: 25 – 35.

Mann M. E. (2002) Little Ice Age. In: The Earth system: physical and chemical dimensions of global environmental change. (ed.) MacCracken M. C. & Perry J. S. Encyclopedia of Global Environmental Change. pp 504 – 509.

Mathijssen P. J. H., Väliranta M., Korrensalo A., Alekseychik P., Vesala T., Rinne J. & Tuittila E-S. (2016) Reconstruction of Holecene carbon dynamics in a large boreal peatland complex, southern Finland. Guaternary Science Reviews. 142: 1 – 15.

McGuire A. D., Anderson L. G., Christensen T. R., Dallimore S., Guo L., Hayes D. J., Heiman M., Lorenson T. D., MacDonald R. W. & Roulet N. (2009) Sensitivity of the carbon cycle in the Arctic to climate change. Ecological Monographs. 17: 523 – 555.

Michaletz S. T., Cheng D., Kerkhoff A. J. & Enquist B. J. (2014) Convergence of terrestrial plant production across global climate gradients. Nature. 512: 39– 43.

Millard A. R. (2014) Conventions for reporting radiocarbon determinations. Radiocarbon. 56: 555–559.

Mitchell E. A. D., Charman D. J. & Warner B. G. (2008) Testate amoebae analysis in ecological and paleoecological studies of wetlands: past present and future. Biodiversity and Conservation 17:2115 – 2137.

Mäkilä M. & Saarnisto M. (2008) Carbon accumulation in boreal peatlands during the Holocene – Impacts of climate variations. In: Peatlands and Climate Change. Strack M. (ed.) International Peat Society. pp. 24 – 43.

Oksanen P. O., Kuhry P. & Alekseeva R. N. (2001) Holocene development of the Rogovaya River peat plateau, European Russian Arctic. The Holocene. 11: 25 – 40.

Oksanen P. O. & Väliranta M. (2006) Palsasuot muuttuvassa ilmastossa – Palsa mires in a changing climate. Suo 57: 33 – 43.

Oksanen J., Guillaume B., Friendly M., Kindt R., Legendre P., McGlinn D., Minchin P. R., O'Hara R. B., Simpson G. L., Solymos P., Stevens H. H., Szoecs E. & Wagner H. (2019) Vegan:

Community Ecology Package. R Package Version: 2.5-6. Webpage: https://cran.r-project.org/web/packages/vegan/vegan.pdf.

PAGES 2k Consortium. (Ahmed M., Anchukaitis K. J., Asrat A., Borgonkar H. P., Braida M., Buckley M. A. J., Büntgen U., Chase M., hristie D. A., Cook E. R., Curran M. A. J., Diaz H. F., Esper J., Fan Z-X. Gaire N. P., Ge Q., Gergis J., Gonzáöez-Rouco J. F., Goosse H., Grab S. W., Graham N., Graham R., Grosjean M., Hanihijärvi A. T., Kaufman D. S., Kiefer T., Kimura K., Korhola A. A., Krusic P. J., Lara A., Lézine A-M., Ljungqvist F. C., Lorrey A. M., Luterbacher J., Masson-Delmotte V., McCarroll D., McConnell J. R., McKay N. P., Morales M. S., Moy A. D., Mulvaney R., Mundo I. A., Nakatsuka T., Nash D. J., Neukom R., Nicholson S. E., Oerter H., Palmer J. G., Phippis S. J., Prieto M. R., Rivera A., Sano M., Severi M., Shanhan T. M., Shao X., Shi F., Sigl M., Smerdon J. E., Solomina O. N., Steig E. J., Stenni B., Thamban M., Trouet V., Turney C. S. M., Umer M., van Ommen T., Verschuren D., Viau A. E., Villalba R., Vinther B. M., von Gunten L., Wagner S., Wahl E. R., Wanner H., Werner J. P., White J. W. C., Yasue K. & Zorita E.) (2013) Continental-scale temperture variability during the past two millennia. Nature Geoscience. 6: 339 – 346.

Palonen V., Pesonen A. Herranen T. Tikkanen P. & Oinonen M. (2013) HASE – The Helsinki adaptive sample preparation line. Nuclear Instruments & Methods in Physics Research. Section B: Beam Interactions with Materials and Atoms. 294: 182 – 184.

Payne R. J. & Mitchell E. A. D. (2009) How many is enough? Determining optimal count total for ecological and palaeoecological studies of testate amoebae. Journal of Paleolimnology. 42: 483 – 495.

Routh J., Hugelius G., Kuhry P., Filley T., Tillman P. K., Becher M. & Crill P. (2014) Multi-proxy study of soil organic matter dynamics in permafrsto peat deposits reveal vulnerability to climate change in the European Russian Arctic. Chemical Geology. 368: 104 – 117.

Sannel A. B. K., Hempel L., Kessler A. & Préskienis V. (2018) Holocene development and permafrost history in sub-arctic peatlands in Tavvavuoma, northern Sweden. Boreas 47: 454 – 468.

Seppälä M. (1986) The Origin of Palsas. Geografiska Annaler. Series A. Physical Geography. 68: 141 – 147.

Seppälä M. (2011) Synthesis of studies of palsa formation underlining the importance of local environmental and physical characteristics. Quaternary Research. 75: 366 – 370.

Siemensma F. (2020) *Placocista spinosa*. Microworld – World of amoeboid organisms. Webpage: https://www.arcella.nl/placocista-spinosa/. (Cited: 25.1.2020)

Sillasoo Ü., Väliranta M. & Tuittila E-S. (2011) Fire history and vegetationrecovery in two raised bogs at the Baltic Sea. Journal of Vegetation Science 22: 1084 – 1093.

Sim T. G., Swindles G. T., Morris P. J., baird A. J., Cooper C. L., Gallego-Sala A. V., Charman D. J., Roland T. P., Borken W., Mullan D. J., Aquino-López M. A. & Galka M. (2021) Divergent responses of permafrost peatlands to recent climate change. Environmental Research Letters 16: 1 – 13.

Slota P. J., Jull A. J. T., Linick T. W. & Toolin L. J. (1987) Preparation of small samples for ^{14}C accelerator targets by catalytic reduction of CO. Radiocarbon. 29: 303 – 306.

Sullivan M. & Booth R. (2007) Key to testate amoebae inhabiting *Sphagnum*-dominated peatlands with an emphasis on taxa preserved in Holocene sediments. Working draft – 21 March 2007. Earth & Environmental Science Department, Leigh University.

Swindles G. T., Holden J., Raby C. L., Turner T. E., Blundell A., Charman J., Menberu M. W. & Kløve B. (2015a) Testing peatland waster-table depth transfer functions using high-resolution hydrological monitoring data. Quaternary Science Reviews. 120: 107 – 117.

Swindles G. T., Morris P. J., Mullan D., Watson E. J., Turner T. E., Roland T. P., Amesbury M. J., Kokfelt U., Schoning K., Pratte S., Gallego-Sala A., Charman D. J., Sanderson N., Garneau M., Carrivick J. L., Woulds C., Holden J., Parry L. & Galloway. (2015b) The long-term fate of permafrost peatlands under rapid climate warming. Scientific Reports. 5: 1 – 6.

Swindles G. T., Morris P. J., Mullan D. J., Payne R. J., Rolands T. P., Amesbury M. J., Lamentowicz M., Turner T. E., Gallego-Sala A., Sim T., Barr I. D., Blaauw M., Blundell A., Chambers F. M., Charman D. J., Feurdean A., Galloway J. M., Galka M., Green S. M., Kajukalo K., Karofeld E., Korhola A., Lamentowicz L., Langdon P., Marcisz K., Mauquoy D., Mazei Y. A., McKeown M. M., Mitchell E. A. D., Novenko E., Plunkett G., Roe H. M., Schoning K., Sillasoo Ü., Tsyganov A. N., van der Linden M., Väliranta M. & Warner B. (2019) Widespread drying of European peatlands in recent centuries. Nature Geosicence. 12: 922 – 928.

Tikkanen P., Palonen V., Junger H. & Keinonen J. (2004) AMS facility at the University of Helsinki. Nuclear Instruments & Methods in Physics Research. Section B: Beam Interactions with Materials and Atoms. 223 – 224: 35 – 39.

Tolonen K. (1966) Stratigraphic and rhizopod analyses on an old raised bog, Varrasuo, in Hollola, south Finland. Annales Botanici Fennici. 3: 147 – 166.

Tolonen K. Warner B. G. & Vasander H. (1992) Ecology if Testaceans (Protozoa: Rhizopoda) in Mires in Southern Finland: I Autecology. Archiv für Protistenkunde. 142: 119 – 138.

Treat C. C., Jones M. C., Camill P., Gallego-Sala A., Garneau M., Harden J. W., Hugelius G., Klein E. S., Kokfelt U., Kuhry P., Loisel J., Mathijssen P. J. H., O'Donnell J. A., Oksanen P. O., Ronkainen T. M., Sannel A. B. K., Talbot J., Tarnocai C. & Väliranta M. (2016) Effects of permafrost aggradation on peat properties as determined from a pan-Arctic synthesis of plant macrofossils. Journal of Geophysical Research: Biogeoscience. 121: 78 – 94.

Turetsky M. R., Manning S. R. & Wieder R. K. (2004) Dating recent peat deposits. Wetlands. 24: 324 – 356.

Turetsky M. R., Abbott B. W., Jones M. C., Anthony K. W., Olefeldt D., Schuur E. A. G., Koven C., McGuire A. D., Grosse G., Kuhry P., Hugelius G., Lawrence D. M., Gibson C. & Sannel A. B. K. (2019) Permafrost collapse is accelerating carbon release. Nature 569: 32 – 34.

Turner T. E., Swindles G. T., Charman D. J. & Blundell A. (2013) Comparing regional and supra-regional transfer functions for palaeohydrological reconstruction from Holocene peatlands. Palaeogeography, Palaeoclimatology, Palaeoecology. 369: 395 – 408.

Turunen J. (2008) Development of Finnish peatland area and carbon storage 1950-2000. Boreal Environment Research 13: 319 – 334.

UNFCCC (2020) The Paris Agreement. Webpage: https://unfccc.int/process-and-meetings/the-paris-agreement/the-paris-agreement. (Cited:9.7.2020)

Vile M. A., Wieder R.K. & Novák M. (1999) Mobility of Pb in *Sphagnum*-derived peat (1999) Biogeochemistry. 45: 35 – 52.

Väliranra M., Blundell A., Charman D. J., Karofeld E., Korhola A., Sillasoo Ü. & Tuittila E.-S. (2012) Reconstructing peatland water tables using transfer functions for plant macrofossils and testate amoebae: A methodological comparison. Guaternary International. 268: 34 – 43.

Warner B. G. (1988) Methods in Quaternary Ecology #5 Testate amoebae (Protozoa). Geoscience Canada. 15: 251 – 260.

Willis K. S., Beilman D., Booth R. K., Amesbury M., Holmqvist J. & MacDonald G. (2015) Peatland paleohydrology in the southern West Siberian Lowlands: Comparions of multiple testate amoebae transfer function, sites and *Sphagnum* $\delta^{13}C$ values. The Holocene. 25: 1425 – 1436.

Young D. M., Baird A. J., Charman D. J., Evans C. D., Gallego-Sala A. V., Gill P. J., Hughes P. D. M., Morris P. J. & Swindles G. T. (2019) Misinterpreting carbon accumulation rates in records from near-surface peat. Scientific Reports. 9:17939.

Yu Z., Beilman D. W., Frolking S., MacDonald G. M., Roulet N. T., Camill P. & Charman D. J. (2011) Peatlands and their role in global carbon cycle. EOS. 92: 97 – 108.

Zhang H., Amesbury M. J., Ronkainen T., Charman D. J., Gallego-Sala A. V. & Väliranta M. (2017) Testate amoebae as palaeohydrological indicators in the permafrost peatlands of north-east European Russia and Finnish Lapland. Journal of Quaternary Science 32: 976 – 988.

Zhang H., Väliranta M., Amesbury M.J., Charman D.J., Laine A. & Tuittila E.-S. (2018a) Successional changes of testate amoebae assemblages along a space-for-time sequence of peatland development. European Journal of Protistology. 66: 36 – 47.

Zhang H., Gallago-Sala A. V., Amesbury M. J., Charman D. J., Piilo S. R. & Väliranta M. M. (2018b) Inconsistent response of Arctic permafrost peatland carbon accumulation to warm climate phases. Global Biogeochemical Cycles. 32: 1605 – 1620.

Zhang H., Piilo S. R., Amesbury M. J., Charman D. J., Gallago-Sala A. V. & Väliranta M. M. (2018c) The role of climate change in regulatin Arctic permafrost peatland hydrological and vegetation change over the last millennium. Quaternary Science Reviews. 182: 121 – 130.